5-1995

Classification of Vegetation and Analysis of its Recent Trends at Camp Williams, Utah Using Remote Sensing and Geographic Information System Techniques

Thomas G. Van Niel
Utah State University

Recommended Citation

CLASSIFICATION OF VEGETATION AND ANALYSIS OF ITS RECENT

TRENDS AT CAMP WILLIAMS, UTAH USING REMOTE SENSING

AND GEOGRAPHIC INFORMATION SYSTEM TECHNIQUES

by

Thomas G. Van Niel

A thesis submitted in partial fulfillment
of the requirements for the degree

of

MASTER OF SCIENCE

in

Watershed Science

UTAH STATE UNIVERSITY
Logan, Utah

1995

ABSTRACT

Classification of Vegetation and Analysis of its Recent

Trends at Camp Williams, Utah Using Remote Sensing

and Geographic Information System Techniques

by

Thomas G. Van Niel, Master of Science

Utah State University, 1995

Major Professor: Dr. R. Doug Ramsey
Program: Watershed Science

Current vegetation classes were generated from remotely

sensed data to provide coarse-level information for an

ecosystem management plan developed at Camp Williams, Utah.

Vegetation trend from 1973-1993 was also examined via

satellite imagery. The data set consisted of Landsat

Multispectral Scanner (MSS) and Thematic Mapper (TM) images

from July or August of 1973, 1975, 1980, 1988, and 1993.

Two approaches were used to detect vegetation change.

The first approach determined overall and cover type trend

from standard digital image differencing of soil-adjusted

vegetation index (SAVI) images. The second approach used an unsupervised classification of a composite SAVI image of all dates.

The first approach defined areas of increase, decrease, and no significant change in SAVI and differences in trend for tree versus shrub cover types. The second approach resulted in an ecological classification that defined new environmental patterns based on vegetation trend.

(148 pages)

ACKNOWLEDGMENTS

CONTENTS

LIST OF TABLES

LIST OF FIGURES

INTRODUCTION

Hydrology is an important component of watershed science, and therefore traditional perspectives of watershed management have concentrated on it. However, land productivity is also important in watershed management; land and vegetation resources need to be managed for goods and services without adversely affecting soil and water resources (Brooks et al., 1991). Since watershed management considers all components of the watershed, including the relationships between land use, soil, vegetation cover, and water (Brooks et al., 1991), the need to examine more than hydrologic characteristics alone is clear.

This thesis will concentrate on the vegetation resources component of watershed science, particularly cover dynamics, to provide information about the complex relationships of vegetation with other physical components of the watershed (e.g., soil and water) and the factors acting upon those components (e.g., land use and disturbance). The possible results include a better understanding of vegetation dynamics (Pickup et al., 1993; Price et al., 1992) and watershed condition and health

(Pickup and Chewings, 1988; Pickup and Nelson, 1984).

Because the analysis of vegetation cover dynamics reveals valuable information about both current and historical environmental characteristics (Neldner and Howitt, 1991; Webb et al., 1970), it is critical in watershed management. Also, the use of satellite remote sensing can provide a historic data base of synoptic coverage for large areas (Hamza, 1986), and generate current and historical conclusions using vegetation analysis (Jackson et al., 1983; Tucker et al., 1985; Bouman, 1992; Price et al., 1992; Hallum, 1993; Pickup et al., 1993). Therefore, remote sensing techniques will be used for vegetation analysis to take advantage of comprehensive sampling of historic data.

A better land management plan could be developed at Camp Williams, Utah with the use of vegetation classification and change detection (cover dynamics) analysis of remotely sensed data along with site specific surveys. A hierarchical multi-scale management plan could help improve the current Land Condition-Trend Analysis (LCTA) natural resource monitoring program at Camp Williams.

This thesis will develop methods for vegetation

analysis from remotely sensed data at Camp Williams and will

be part of coarse-scale analysis of the hierarchical

ecosystem management plan being developed at the camp.

Vegetation patterns can provide a more comprehensive context

for analyzing important environmental issues such as fire

behavior prediction, ecological status, and wildlife and

livestock concerns at Camp Williams.

LITERATURE REVIEW

LAND MANAGEMENT

Current pressure from both public views and government policy concerning environmental issues holds land managers more accountable for land-use decisions than ever before (Kessler et al., 1992). Wildland uses and values are now viewed in a larger context and require an interdisciplinary research environment to adaptively manage the land (Kessler et al., 1992).

This motivates land management agencies to improve their policies such that they consider land use activities as well as ecosystem health at a number of scales (Kessler et al., 1992). The Department of Defense (DOD), to improve their environmental management, is currently establishing an ecosystem-level management plan.

Natural resource evaluation of DOD land is currently based on the LCTA program (Tazik et al., 1992). LCTA depends on site-specific sampling of fixed environmental plots, e.g., 100-meter transects that, once established, are monitored every year to determine both land condition and

trend. Transect location is determined from a spectral
classification of a satellite image and soil information.
Only areas that are homogeneous in both spectral class and
soil class are considered for transect placement.
Heterogeneous areas of land are not considered for LCTA
monitoring.

The LCTA program has come under criticism because of
its approach; the theoretical basis of the program is
unknown and the sampling scheme excludes much of the
ecosystem (e.g., possibly critical mixed vegetation and soil
areas) (West et al., 1994). There is no indication that the
LCTA contains any scientific method for determining the
number of spectral classes needed to address landscape
variability; instead, a fixed number of spectral classes is
used for all LCTA locations (Tazik et al., 1992). Unless
the number of spectral classes is determined using a
scientifically repeatable method or related to actual
environmental classes, analysis may be ideosyncratic. This
is true because environmental complexity caused by
geographic location, patch size and shape, cumulative
effects, and site characteristics makes identification of

spectral classes a site-specific attribute. When spectral classes are determined without such consideration (as in LCTA), boundaries may be arbitrary, and results of analysis deceptive.

Not only does the LCTA program purposefully ignore high diversity areas that may be important, but it may unintentionally miss critical areas because of the sampling method used; boundaries may include spectrally similar areas that are ecologically distinct or it may split types that are ecologically similar. Either way, the LCTA program is in need of modifications that consider the entire landscape, and have a scientific basis (e.g., cover dynamics). This cumulative landscape analysis may be accomplished using both remote sensing and geographic information system (GIS) technologies and can be tied to the more specific LCTA monitoring.

Recently, GIS's have become a key tool used to integrate management practices and help produce ecosystem management plans. The integration of remote sensing and GIS technologies have been used extensively for vegetation mapping (Franklin, 1989; Franklin and Peddle, 1987; Franklin

and Wilson, 1991; Neldner and Howitt, 1991; Eidenshink,

1992; Ramsey et al., 1992) and characterization of

vegetation dynamics (Hallum, 1993; Pickup et al., 1993;

Price et al., 1992).

LAND COVER MAPPING

Defining accurate environmental boundaries has been a

continuing scientific endeavor important in environmental

management (Bailey, 1985; Eidenshink, 1992; Küchler, 1964).

Delineating boundaries by factors that control the

distribution of vegetation (i.e., climate) to produce climax

vegetation or habitat type associations rather than the

product of these controlling factors (the vegetation itself)

generally results in static boundaries (Bailey, 1985;

Clements, 1936). By using the controlling factors,

ecosystem boundaries are identified regardless of present

land use or existing vegetation and are indicative of

natural vegetation without human interference (Bailey,

1985); however, there is a strong contrary argument that

there are no absolute controlling factors over vegetation or

the environment, and to assume so is misleading (Webb et

al., 1970). There is too much natural variability,

fluctuation, and cumulative environmental change to permit

the identification of a single controlling factor on the

environment (Gleason, 1926; Webb et al., 1970). In fact

Gleason (1926, p.96) stated that for practical purposes the

only measure of the environment is its result, as expressed

in plant life." This indicates the importance of a current

actual vegetation map in environmental management.

The climax association method stresses temporal

dynamics of plant communities, but ignores spatial patterns

of vegetation (O'Neill et al., 1986). The climax

association method, therefore, has limited use in any

intensive management because it ignores the vegetation that

is present and predicts only the potential natural

vegetation. These potential vegetation classes or habitat

types (Clements, 1936) may apply to large areas to some

degree, but they do not predict with any certainty what the

vegetation is at a particular site at a given time (Urban et

al., 1987). Knowledge of putative climax vegetation can

lead to estimates regarding productivity of tree stands,

cutting intervals, and relations between animal species

(Winn, personal communication, 1993), but without knowledge of actual vegetation, management is severely restricted; the climax type may be the same for sites that are physically very different and need to be managed differently. Although knowledge of habitat type or climax association has been more efficient in the past for mapping large areas because of its temporal longevity, remote sensing technology now allows large areas to be mapped for actual vegetation (Eidenshink, 1992; Ramsey et al., 1992).

Knowledge of current vegetation type is useful for management and can be used in conjunction with habitat types to define present spatial pattern and ecosystem structure. Remotely sensed imagery contributes to this process because it provides an overview of an area at one instant in time. Classification of remotely sensed data, like most mapping procedures that model actual vegetation, emphasizes spatial patterns without including temporal dynamics (O'Neill et al., 1986); however, these temporal problems can be partly overcome by developing sets of remotely sensed data over several years. This approach has the advantages of both spatial and temporal consideration, and usefulness in

management (Eidenshink, 1992). Current vegetation type is more practical in management situations than climax association or habitat type because it is representative of a "dynamic equilibrium" over a period of time (Eidenshink, 1992), and is, therefore, more helpful when connections between different scales are analyzed for management as in an ecogeographical analysis.

Ecogeographical analysis is the subdivision of a landscape into ecosystems at different levels of detail that can be linked to different levels of analysis (Bailey, 1988). The practical value of this analysis is to stratify ecosystem productivity or probable responses to management practices (Bailey, 1983). These benefits of a hierarchial mapping system can be achieved at coarser scales using remote sensing and at finer scales by site-specific surveys. Data sets from these studies can be entered into a GIS and used to manage, monitor, and model vegetation information.

The usefulness of the spatially focused current vegetation approach can be enhanced by a hierarchial method, which takes advantage of linkages and connectivity of scales. This approach can be made more appropriate for

management by using time series data allowing for historical analysis of general ground cover trends.

VEGETATION ANALYSIS USING REMOTE SENSING

The objective of vegetation analysis from spectral measurements is to reduce the spectral data to a single number that is related to physical characteristics of vegetation (e.g., leaf area, biomass, productivity, photosynthetic activity, and percent cover) (Perry and Lautenschlager, 1984; Huete, 1988; Baret and Guyot, 1991), and to minimize the effect of internal (e.g., canopy geometry, and leaf and soil properties) and external factors (e.g., sun angle, and atmosphere) on the spectral data (Richardson and Wiegand, 1977; Slater and Jackson, 1982; Kimes, 1983; Huete et al., 1985; Huete, 1987; Chavez, 1988; Singh, 1989; Huete and Warrick, 1990; Baret and Guyot, 1991; Huete and Escadafal, 1991; Gong et al., 1992; Li et al., 1993). Vegetation indices (VI's) developed in an attempt to obtain this objective have serious limitations (Huete et al., 1985; Huete, 1987; Huete and Jackson, 1987; Huete, 1988; Huete and Warrick, 1990; Baret and Guyot, 1991; Huete

et al., 1992). Qi et al. (1993) found atmosphere, view, and soil background influences on VI's to be complex and dependent on surface conditions.

VI's are separated in the form of linear combinations (orthogonal) and ratios (Perry and Lautenschlager, 1984; Huete et al., 1985; Baret and Guyot, 1991). Kauth and Thomas (1976) developed a four-band "tasseled cap" orthogonal transformation that uses the four MSS bands to create four indices called: (1) soil brightness index (SBI), (2) green vegetation index (GVI), (3) yellowness index (YI), and (4) non-such index (NSI) (Jensen, 1986). Each of the four MSS bands are multiplied on a pixel-by-pixel basis by the appropriate tasseled cap coefficient; these values are then added together (Jensen, 1986; Kalcic, 1980). For example, the equation for the GVI is:

$$GVI = (C1)green + (C2)red + (C3)NIR6 + (C4)NIR7$$

where C1-C4 represent tasseled cap coefficients and green, red, NIR6, and NIR7 represent MSS bands 4-7, respectively.

Yellowness is sensitive to haze whereas non-such is sensitive to water vapor absorption. Both were shown to be independent of vegetation changes (Jackson et al., 1983).

Indices of greenness and brightness are helpful in interpretation of vegetation.

The perpendicular vegetation index (PVI) of Richardson and Wiegand (1977) used two Landsat bands (NIR and red) to develop a measure of brightness and greenness:

$$PVI = ((Rgg5 - Rp5)^2 + (Rgg7 - Rp7)^2)^{\frac{1}{2}}$$

where Rp is the reflectance of a candidate vegetation spot for Landsat bands MSS5 and MSS7, and Rgg is the reflectance of soil background corresponding to a candidate vegetation spot (Richardson and Wiegand, 1977).

The soil line is a two-dimensional variation of the Kauth-Thomas SBI, and a plot of NIR and red (MSS7 and MSS5) shows that soils fall on this straight line (Jensen, 1986; Richardson and Wiegand, 1977). Presence of vegetation causes the red radiance to decrease because of strong absorption in the visible region by chlorophylls (Knipling, 1970). NIR radiance increases with the presence of vegetation due to internal leaf scattering and no absorption by chlorophylls in the NIR spectral region (Knipling, 1970). The orthogonal distance between the soil line and the vegetation spot is a measure of the amount of vegetation

(Richardson and Wiegand, 1977). This principle remains the same for n-space indices greater than two. The third dimension (yellowness) is measured orthogonally to both brightness and greenness, and the fourth dimension (non-such) is mutually orthogonal to brightness, greenness, and yellowness (Jackson, 1983).

These n-space indices were thought to be particularly useful for discriminating vegetation from soil background (Jackson, 1983), but Huete et al. (1985) showed that normalization of the soil background to a one-dimensional soil line only removes the bare soil spectral influences (differences due to soils of different types in the same brightness range) and not the greater soil brightness influences. Thus GVI and PVI are sensitive to background soil effects that can seriously alter vegetation readings (Huete et al., 1985; Huete and Jackson, 1987; Huete, 1988).

Ratio indices such as the ratio vegetation index (RVI), and the normalized difference vegetation index (NDVI) of Rouse et al. (1973), and the transformed normalized difference vegetation index (TNDVI) of Deering et al. (1975) use various ratios of red and near-infrared bands to

determine presence of vegetation:

$$RVI = NIR / red,$$

$$NDVI = (NIR - red) / (NIR + red), \text{ and}$$

$$TNDVI = (NDVI + 0.5)^{\frac{1}{2}}.$$

These indices are widely used, though they also suffer from background soil interference. The RVI is soil dependent and is sensitive to differences in sunlit and shaded soil components resulting from deviations from the solar zenith angle, making it a gross and unreliable measure of leaf area index (LAI) and biomass (Huete, 1987; Sellers, 1985). The NDVI and the TNDVI are also influenced by sun angle changes and are affected by soil background to the point that they are as sensitive to soil darkening as to vegetation development (Huete, 1987; Huete and Jackson, 1987; Huete, 1988). Soil background influences cause greenness lines to be nonparallel (Huete et al., 1985). In other words, for equal vegetation densities, the vegetation index value can vary greatly depending on the soil background. In fact, TNDVI and NDVI values can range from 20% to 55% for a static vegetation density over a dynamic soil background (Huete et

al., 1985). This can be very detrimental to any analysis of vegetation.

Since soil background conditions influence the spectral values of partial canopies and, therefore, the vegetation indices calculated from these spectra (Huete, 1988; Richardson and Wiegand, 1977), the vegetation trend analysis at Camp Williams must account for these soil effects. Huete et al. (1985) showed that soil-vegetation spectra were best approximated by the PVI at low vegetation densities and by the RVI at higher densities. However, at intermediate vegetation levels, neither index is adequate. In fact, because neither ratio nor orthogonal indices can adequately describe intermediate densities of vegetation, almost any index adjustment for soil would improve remotely sensed vegetation interpretation (Huete, 1988).

The soil-adjusted vegetation index (SAVI) was designed to compensate for VI limitations by normalizing sunlit and shaded soil differences across all viewing angles and minimize dry and wet soil variations (Huete, 1987; Huete et al., 1992). However, SAVI has also been shown to be affected by atmosphere and view direction variations (Qi et

al., 1993). SAVI has, on the other hand, minimized temporal and spatial soil differences due to wetting compared to the NDVI, making it a better index over partial canopies (Qi et al., 1993). This index is given by:

$$SAVI = [(NIR - red) / (NIR + red + L)] * (1 + L).$$

VI's, when plotted from the NIR-red space origin, reveal lines of equal values called isolines (Figure 1) (Huete, 1988). If vegetation isolines do not correspond with the isolines predicted by the VI, the difference is partly due to soil background influence; different soil backgrounds under constant vegetation produce different VI brightness values (Huete, 1988). The SAVI is very similar to the NDVI except that an adjustment factor (L) is included into the equation so vegetation is better represented by the VI isolines (Huete, 1988).

Huete (1988) showed that the vegetation isoline behavior is better predicted by shifting the NIR-red space origin to a point where intermediate vegetation densities converge with the soil line (approximate isoline convergence point Figure 1 (E)). Figure 1 reveals a partial canopy over
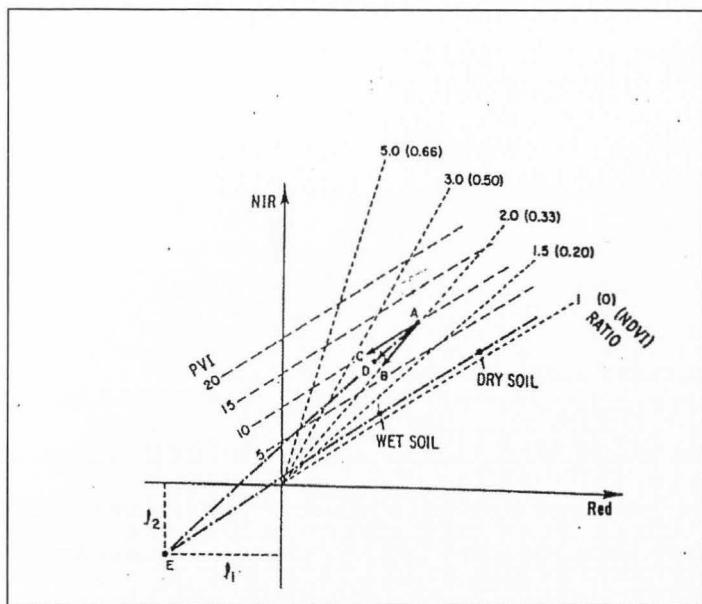
Fig. 1. Vegetation isolines in NIR-red wavelength space predicted from the normalized difference-, and perpendicular-vegetation indices (from Huete, 1988).

a dry soil (A), its shift along an NDVI isoline (B), and its shift along a PVI isoline (C).

The intersection of the bisection of AB and AC (D) and the soil line forms the approximate isoline convergence point (E). This shifting of the origin toward negative

values is the same as adding a constant (L) to the NIR and red reflectance values (Huete, 1988). Optimal adjustment factors were empirically found to depend on vegetation densities, but it was shown that for any adjustment factor between 0.25 and 1.0, soil influences were considerably reduced in comparison to the NDVI or PVI (Huete, 1988). In fact, an adjustment factor of 0.5 should reduce soil-induced variations and improve the linearity between the spectral index and vegetation characteristics when compared to the NDVI (Huete, 1988). Huete (1988) showed that a lower amplitude exists for the SAVI when compared to the NDVI, but vegetation discrimination and soil noise levels were considerably improved.

OPTICAL REMOTE SENSING

A basic understanding of the electromagnetic (EM) spectrum and its interaction with the atmosphere and earth surfaces is important in a study using optical remote sensing and is given by Goetz et al. (1985) among others. VI's developed from spectral measurements are based on known characteristics of the reflectance of radiation from

vegetation in both the visible and NIR parts of the EM

spectrum. These characteristics are considered in defining

VI's to exploit differences in the reflectance patterns of

green vegetation compared to other objects (Perry and

Lautenschlager, 1984). Therefore, the physical and

physiological basis behind vegetation canopy reflectance

(Knipling, 1970; Colwell, 1974; Sellers, 1985; Sellers,

1987), and leaf reflectance (Knipling, 1970; Gausman, 1974)

of radiation should be understood.

Idealized reflectance patterns for vegetation and soil

are given in Perry and Lautenschlager (1984). Dead

vegetation usually has higher reflectance in the visible

part of the EM spectrum and lower reflectance in the NIR

part of the EM spectrum than live vegetation; soil typically

has higher reflectance than live vegetation but lower than

dead vegetation in the visible and has lower reflectance

than both live and dead vegetation in the NIR portion of the

EM spectrum (Perry and Lautenschlager, 1984).

CHANGE DETECTION

Vegetation trend, particularly cover dynamics, is very important in ecological studies because it can provide information about landscape processes and ecological status (Pickup et al., 1993; Webb et al., 1970). However, to detect a valid change over time, standardization of values from different satellites, with differences in illumination, and atmospheric conditions must be completed (Pickup et al., 1993).

Once standardization is complete, a difference image is created by spatially registering at least two images (e.g., VI images) acquired at different times and then subtracting one image from the other on a pixel-by-pixel basis (Gong et al., 1992). The distribution of the difference image is approximately Gaussian in nature; pixels of no (brightness) change are distributed around the mean and pixels of change are found in the tails of the distribution (Jensen, 1986). One standard deviation from the mean is often used as the threshold value, which determines the boundary between change and no change; this threshold, however, can be tested

empirically to determine if it is the best boundary to accurately define change (Jensen, 1986).

Coarse-level vegetation analysis should serve as a first step in developing a land management plan. A current vegetation map and vegetation change analysis can help determine vegetation status over the past 20 years and define areas of change versus no change at Camp Williams. This level of analysis increases knowledge of landscape processes considering the entire camp, and can be connected to the more specific scale of analysis (including LCTA). Most importantly, it can make land management more cost effective. Location and intensity of site specific surveys should be determined after consideration of change detection classes; stable and unstable areas may require different levels of monitoring.

THE CAMP WILLIAMS PROJECT

In 1993, to provide a better management plan for Camp W. G. Williams Utah National Guard Training Area, Utah State University, in collaboration with military personnel at Camp Williams, established an interdisciplinary ecosystem

research project. The project is separated into seven interrelated tasks including: (1) a survey of flora, (2) a survey of fauna, (3) LCTA, (4) range utilization, (5) fire ecology, (6) soils characterization , and (7) development of a GIS.

OBJECTIVES

The objectives of my research were to generate a current vegetation map and to determine land cover trends from 1973 to 1993 at Camp Williams using remote sensing techniques. In order to determine the changes in vegetation that have occurred since 1973, the two objectives were:

1. To accurately classify vegetation from 1993 Landsat TM imagery of Camp Williams, Utah, and

2. To determine whether there has been ground cover change at Camp Williams, Utah since 1973.

JUSTIFICATION

These objectives can be justified on the basis that new approaches are required to sustain or improve the current management system of military installations. Baseline data are provided in the form of a vegetation map (from objective one) and ground cover dynamics maps (from objective two).

Since LCTA is new to several military reservations (including Camp Williams), land condition and trend data are available for only a few years. Completion of objective two can improve management of the camp by defining areas as to degree of change from 1973 to 1993. This permits a more cost-effective and intelligent management plan to be initiated; areas of lesser to no change may require less intensive monitoring than areas of rapid, pronounced change. Such synoptic coverage also provides data for years past that have not been monitored.

The results of these objectives enhance current and historical knowledge of Camp Williams and should allow for better management of the camp by complimenting the current LCTA program with synoptic coverage and an ecological

theoretical basis (e.g., vegetation dynamics). The sampling

scheme herein includes the entire landscape, outlines a

model by which historical analysis of other military

training facilities could proceed, and provides a new

approach for stratifying land within military reservations.

STUDY SITE

Camp Williams, Utah was declared a federal military reservation in 1914, but has been used for encampments since 1854. Since its initiation, Camp Williams has been subject to increasing amounts of human-related impacts, but little environmental management has taken place until recently. The camp provides support for several military and civilian activities at the federal, state, and local levels, which create a variety of land-use activities within the camp boundaries. Land uses include specialized winter, desert, mountain and amphibious training; numerous firing ranges; public youth camp activities; agriculture; and sheep and cattle grazing.

Camp Williams occupies 25,000 acres on the southern end of Salt Lake Valley in north central Utah. The camp is situated on the western portion of the Traverse Mountains, which range in elevation from approximately 4200-7200 feet above sea level. Alluvial fans from the adjoining Oquirrh Mountains overlie terrace soils of Pleistocene Lake

Bonneville to form a geologically complex mosaic (Shultz, 1993).

Vegetation on and around the camp is dominated by oakbrush and tall shrubs at upper elevations, and sagebrush/grass communities at lower elevations. Figure 2 reveals phasic developement of forbs, grasses, and shrubs for a site representing the sagebrush/grass vegetation type.

The temperate desert climate at Camp Williams averages 11 inches (279.4 mm) of precipitation annually with most falling as snow in the winter (Shultz, 1993). Figure 3 shows total precipitation from October through June for 1966-1993 to reveal precipitation from the beginning of the water year up to satellite acquisition dates. Figures 4-8 show the precipitation from October through June for satellite acquisition years (1973, 1975, 1980, 1988, and 1993, respectively).
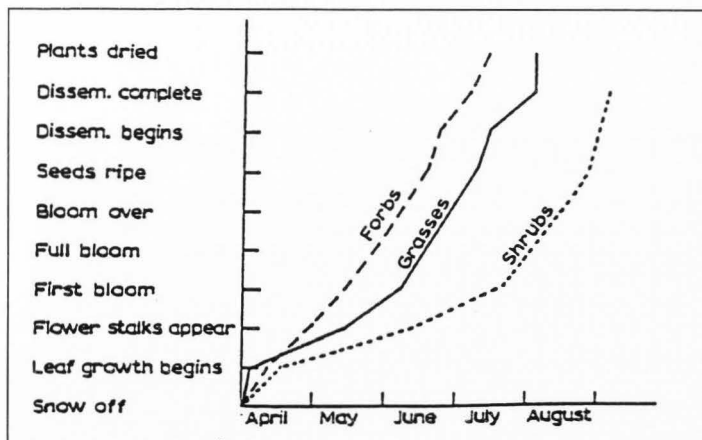
Fig. 2.   Average development of grasses, forbs, and shrubs at the U.S. Sheep Experiment Station, Dubois, Idaho, 1941-47 (from Blaisdell, 1958).
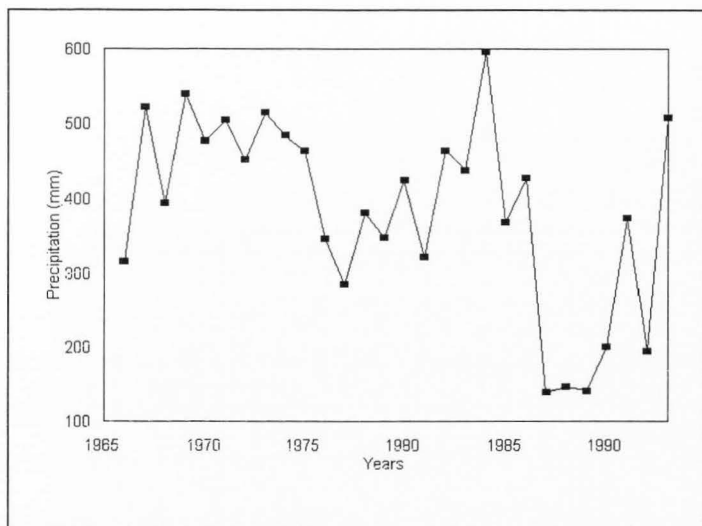
Fig. 3. Total annual precipitation from October-June for 1966-1993 at Camp Williams.
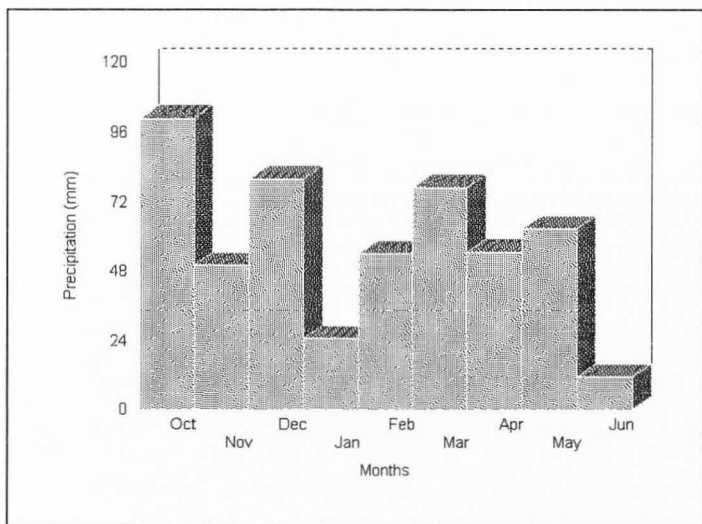
Fig. 4. Precipitation from October-June for 1973 at Camp Williams.
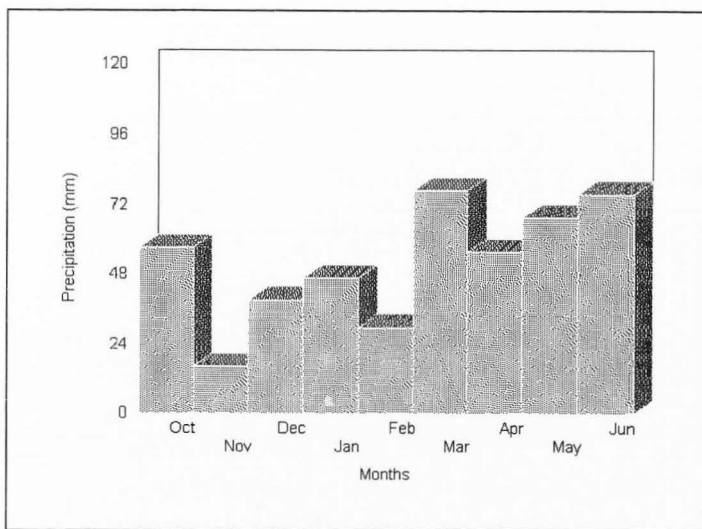
Fig. 5.   Precipitation from October-June for 1975 at Camp
Williams.
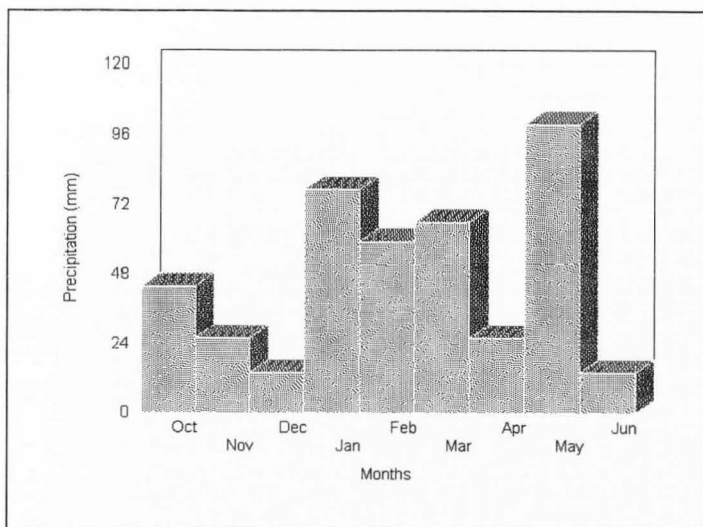
Fig. 6. Precipitation from October-June for 1980 at Camp
Williams.
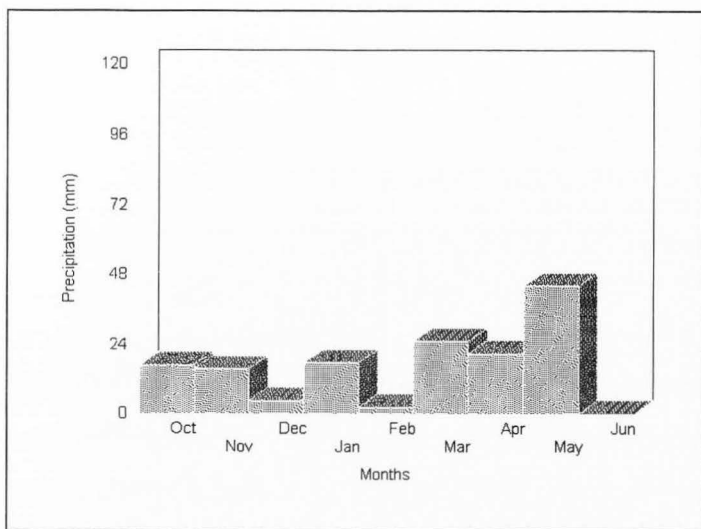
Fig. 7.   Precipitation from October-June for 1988 at Camp Williams.
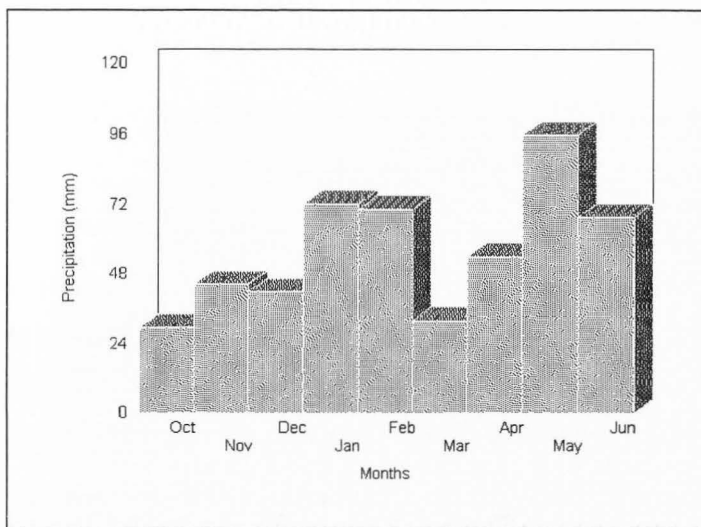
Fig. 8.   Precipitation from October-June for 1993 at Camp Williams.

METHODS

Three Landsat Multispectral Scanner (MSS) and two Thematic Mapper (TM) images were acquired for five dates over a twenty year time period (Table 1). A 1993 TM image was used to classify current land cover and land-use classes at Camp Williams, Utah and two approaches were used to determine vegetation trend on these images.

The first approach used standard digital image differencing on a multitemporal dataset of SAVI images to determine overall and per cover type trend. Image differencing for all combinations of years determined overall trend for the camp while cover type polygons generated from the classification of 1993 TM imagery allowed vegetation trend to be summarized by cover type.

The second approach used an unsupervised classification technique on a composite image of all dates (five bands, each consisting of a SAVI image from a different year). The resulting signatures were expected to reveal vegetation trends.

TABLE 1. SATELLITE IMAGE INFORMATION FOR THE CAMP WILLIAMS
DATA SET.

Image Date	Sun Elevation Angle	Landsat Number	Scanner
06/27/1973	29	1	MSS
06/26/1975	31	2	MSS
07/05/1980	32	2	MSS
08/23/1988	39	5	TM
07/20/1993	33	5	TM

All images were standardized to account for differences
in atmospheric effects, radiometric calibration, scene
illumination, soil background effects, and image
registration. Direct substitution of TM band 3 (Red) and 4
(NIR) for MSS band 2 (Red) and 4 (NIR) was used to compare
between TM and MSS images (Crist and Cicone, 1984).

ATMOSPHERIC CORRECTION

The histogram minimum method was used to deal with simple haze correction differences of the atmosphere for each image (Chavez, 1975; Jensen, 1986). This method ignores atmospheric absorption, which is difficult to determine because of its dependence on water vapor in the atmosphere (Jensen, 1986). Generally, increased atmospheric scattering takes place in the visible bands, resulting in higher brightness values, whereas increased atmospheric absorption results in lower brightness values in the longer infrared and reflected NIR bands (Jensen, 1986). A bias value was subtracted from each band on a pixel-by-pixel basis, resulting in left-shifted histograms with minimum values of zero (Jensen, 1986).

**RADIOMETRIC CALIBRATION AND SCENE
ILLUMINATION CORRECTION**

For all images, the digital counts in each band were put back through the "lookup" tables located on the computer compatible tape's (CCT) header files. These "lookup" tables contain information on any radiometric adjustments made to the data; the data were converted directly to radiometric

counts and changed to decompressed mode using prelaunch calibrations (Pickup et al., 1993).

Radiance values and sun elevation angles were downloaded to calculate gains and biases, and correct for illumination effects, respectively. These values were used to radiometrically calibrate for differences in satellites by converting digital numbers (DN's) to surface reflectance values (Robinove, 1982; Singh, 1985a; Singh, 1985b; Teillet, 1986; Markham and Barker, 1987; Slater et al., 1987; Chavez, 1989; Holm et al., 1989; Moran et al., 1992). Appendix A has a detailed explanation of this standardization process.

SOIL BACKGROUND EFFECTS

Soil background effects in change detection (approaches 1 and 2) were not eliminated, but were minimized by using SAVI (Huete, 1987; Huete et al., 1992; Qi et al., 1993).

IMAGE REGISTRATION

All images were geometrically rectified into the UTM coordinate system using ground control points (GCP's) that were visibly distinct throughout the Landsat scene. A least squares method was used to calculate the transformation from

the image to a planar map. A first-order linear
transformation was used. This took into account seven kinds
of distortion in the image (location in x and/or y, scale in
x and/or y, skew in x and/or y, and rotation) and is
expressed in root mean square error (RMS). The acceptable
RMS error threshold value was 1 for TM images and 0.5 for
MSS images. This means that the acceptable distance between
map location and image location is one pixel or not above 30
meters for Landsat TM, and one half pixel or about 40 meters
for Landsat MSS.

**LAND USE/LAND COVER TYPE
CLASSIFICATION**

A TM image (20 July 1993) was acquired over Camp
Williams for the classification of cover types. A semi-
supervised classification approach was used to identify
plant community types. A nonparametric ISODATA clustering
algorithm generated thirty spectral clusters (Campbell,
1987). These spectral clusters were used to classify the
imagery using a maximum likelihood classification. A
maximum likelihood classifier considers the mean as well as
the variability of brightness values in each spectral

cluster to calculate probabilities of pixel membership to each of the ISODATA clusters (Campbell, 1987). The variation present within spectral clusters and the problems that may arise when spectral value distributions from separate clusters overlap were taken into account (Campbell, 1987).

The original thirty spectral classes were merged into twelve cover type classes by relating them to ground cover data (Figure 9). This was accomplished using spectral signature analysis, aerial photography, videography, and digital elevation models (DEM).

Seven of the twelve land use/land cover classes are included in the vegetation cover trend analysis. These are (1) oakbrush, (2) sagebrush, (3) juniper, (4) oakbrush-sagebrush-grass mix, (5) grass sparse shrub, (6) bare/annual weed, and (7) agriculture.

IDENTIFICATION OF COVER CHANGE

In collaboration with the fire ecology study of the Camp Williams project, areas of recent, pronounced ground cover change (burns) have been identified along with the
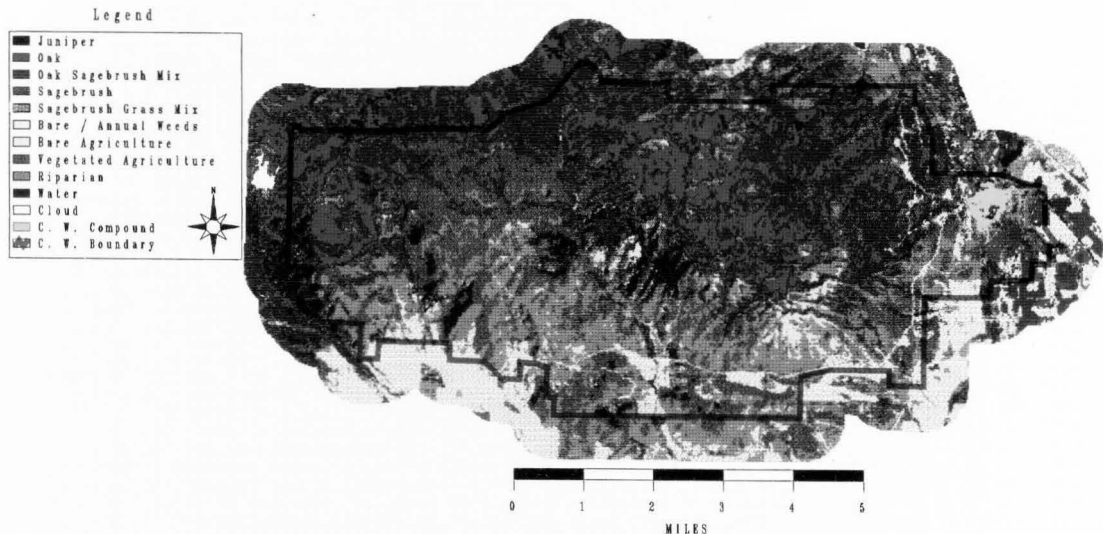
Fig. 9. Land cover/land use map of Camp Williams, Utah. An unsupervised classification approach was used to identify thirty spectral clusters. Aerial photos, digital elevation models (dems), and spectral signature analysis were used to combine clusters into land cover/land use classes.

42

approximate date of change as seen in Figure 10 and Table 2.

These data provide a history and validation of cover change.

The fire boundaries were delineated using a Trimble GPS and

dated by growth ring analysis of several oakbrush stems

within the fire boundaries (Godfrey, 1995).

ANTECEDENT PRECIPITATION INDEX

In a study of Utah rangelands, Dugas (1980) found that

soils at his sites generally began the growing season with a

fully water-saturated profile that were depleted by

midsummer. It was the interannual variations in soil

moisture, however, that greatly influenced plant response

(timing of occurrence or nonoccurence of phenological stages

or magnitude of production) (Dugas, 1980). The variation in

growing season soil moisture at Camp Williams, and

subsequent influence on vegetation, was considered to

provide more information about the vegetation measurements

of the satellite imagery.

Since direct measurements of actual antecedent soil

moisture data were not available for Camp Williams, an

antecedent precipitation index (API) was used to quantify
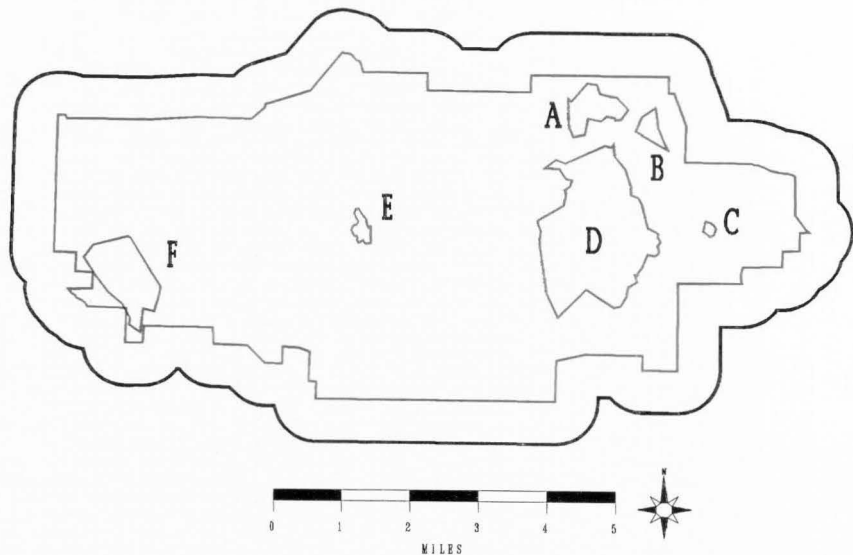
Fig. 10. Mapped fire boundaries. Fire boundaries were delineated using a global positioning system (GPS) in the summer of 1993. The fires were dated using growth ring analysis of several oakbrush stems within fire boundaries.

44

TABLE 2. SIZE AND YEAR OF RECENT FIRES AT CAMP WILLIAMS
NATIONAL GUARD BASE, UTAH.

Fire	Size (hectares)	Year
A	95.44	1987
B	30.59	1990
C	7.25	1992
D	718.67	1987
E	22.34	1988
F	203.92	1976 and 1978

soil moisture. API's have received widespread use because
they are based on precipitation data, which are readily
available and directly related to moisture deficiency of
basins (Viessman et al., 1977). API values were calculated
for March 1 through satellite acquisition dates for 1973,
1975, 1980, 1988, and 1993 (Figures 11-15).

The API is calculated daily and includes an
exponentially decreasing recession contant (K = 0.9), which
considers timing of precipitation; the weight of any
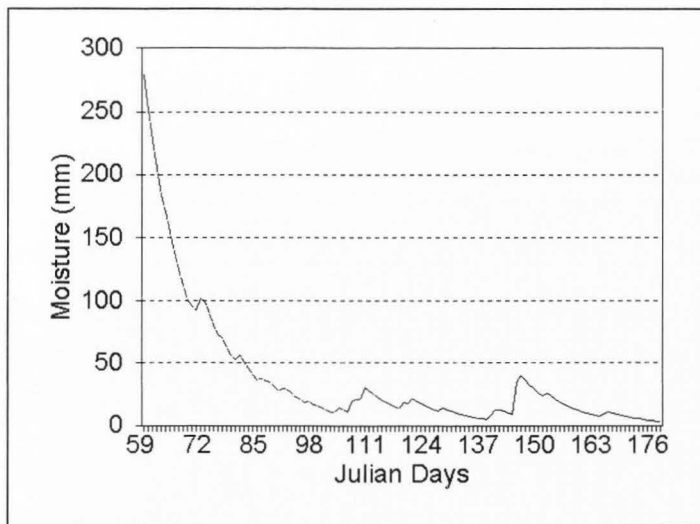
Fig. 11. Antecedent precipitation index (API) for 1973 at
Camp Williams. API is a precipitation based measure of soil
moisture.
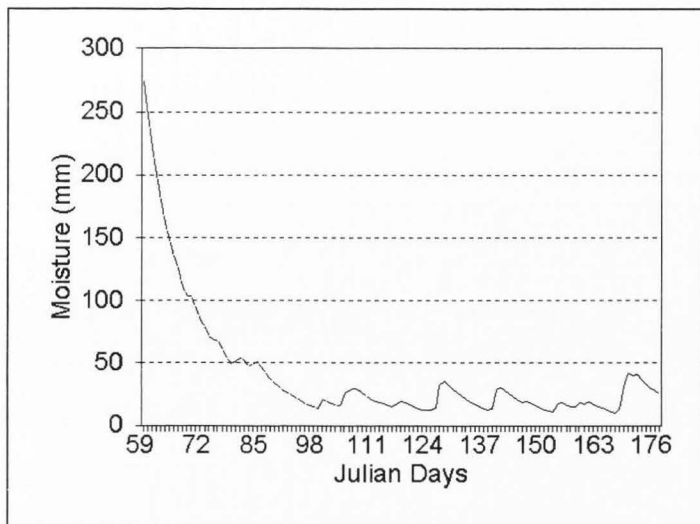
Fig. 12.   Antecedent precipitation index for 1975 at Camp Williams.
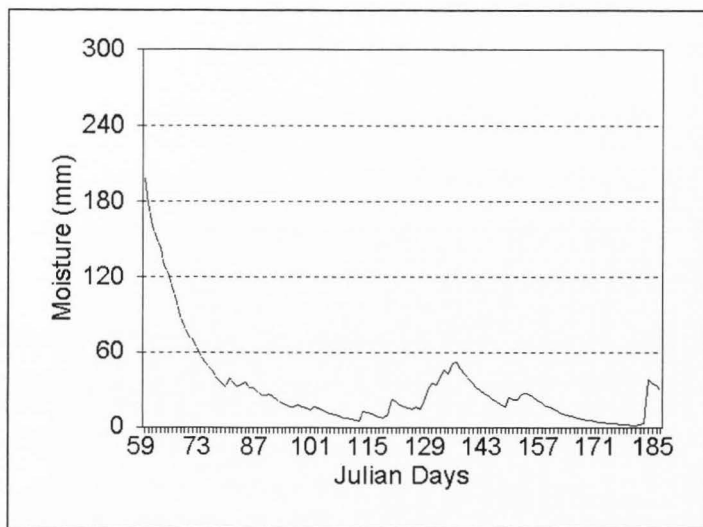
Fig. 13.   Antecedent precipitation index for 1980 at Camp
Williams.
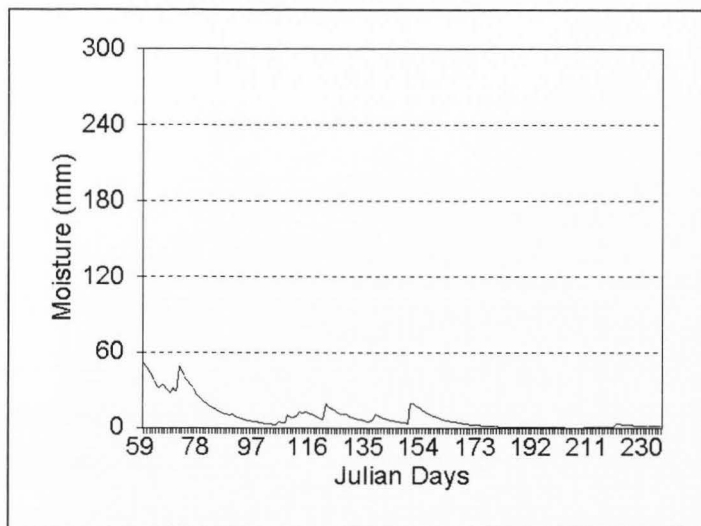
Fig. 14. Antecedent precipitation index for 1988 at Camp Williams.
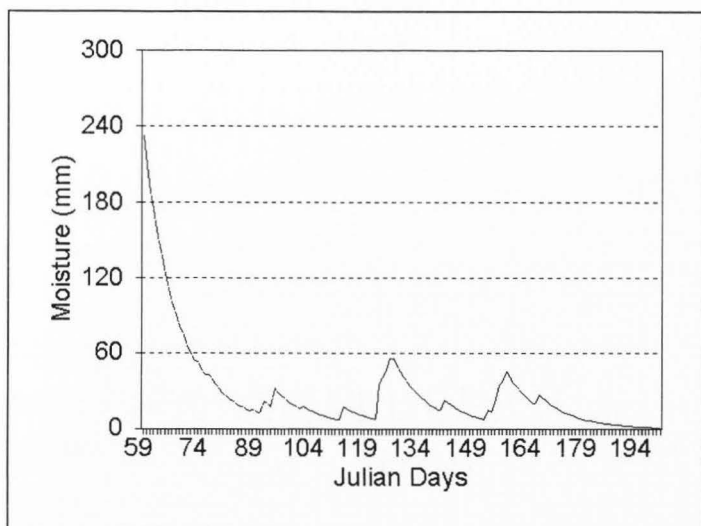
Fig. 15.   Antecedent precipitation index for 1993 at Camp
Williams.

precipitation event in an API calculation decreases as time
progresses. The API was not meant to be a complex
representation of soil moisture at Camp Williams, but rather
a simple model to provide more information for analysis.
For a detailed explanation of this process, see Apendix B.

IMAGE DIFFERENCING

Overall Image Difference

SAVI images were created from each of the five
standardized TM and MSS images (1973, 1975, 1980, 1988, and
1993). A soil adjustment constant (L) of 0.5 was used for
all images. All possible date combinations of image
differences were generated (Figure 16).

SAVI images were also created for all the images using
a soil adjustment constant (L) based on the API (SAVI API).
As the soil background becomes more wet, L should become
smaller, and as the soil becomes drier, L should become
larger (Figure 1). This corresponds to characteristics of
vegetation canopy reflectance. Soil darkening under a
vegetation canopy decreases the amount of red reflectance

A. 1993 - 1988

F. 1988 - 1975

B. 1993 - 1980

G. 1988 - 1973

C. 1993 - 1975

H. 1980 - 1975

D. 1993 - 1973

I. 1980 - 1973

E. 1988 - 1980   Legend   J. 1975 - 1973

Negative Change (below -1 st. dev.)
No Change (-1 to 1 st. dev.'s)
Positive Change (above 1 st. dev.)

0 1 2 3 4 5
MILES
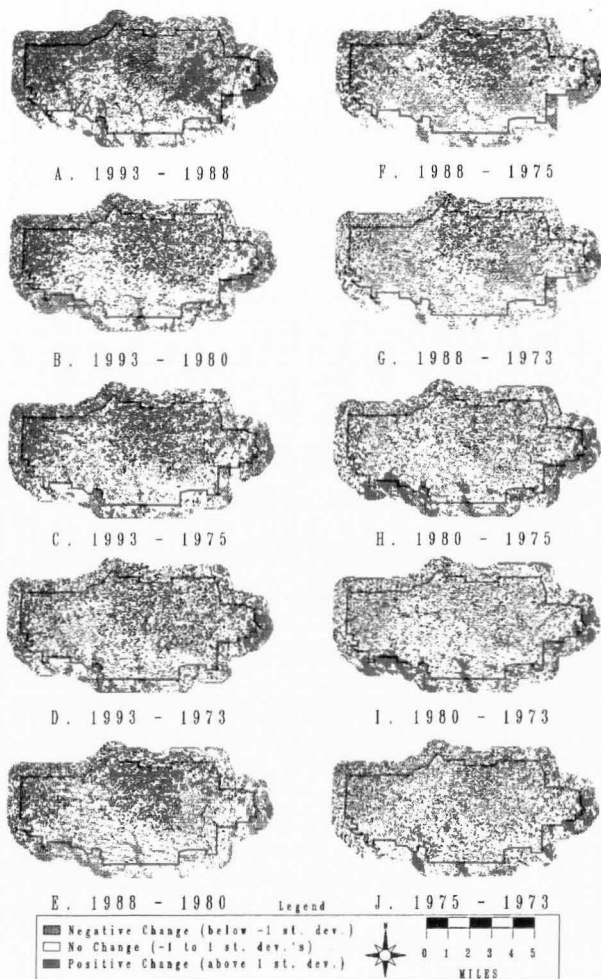
Fig. 16.   Image differences at Camp Williams, Utah.   Green areas have increased in SAVI and brown areas have decreased in SAVI.

This increases the numerator of the VI and considerably more than the NIR reflectance (Colwell, 1974). overestimates the amount of vegetation. To compensate, a smaller L will theoretically lower the VI calculation to a more representative vegetation measure.

All SAVI API difference image combinations were subtracted from SAVI combinations (with L = 0.5) to determine if there was a measureable difference (Figure 17). A detailed explanation of SAVI API generation is given in Appendix C.

Cover-Type Difference

Cover-type polygons generated from the land use/land cover classification of the 1993 TM (Figure 9) image were used to determine change relative to vegetation type. All dates were differenced from the 1993 data set to look at change relative to the date used to generate the land use/land cover map (Figures 18-24). Other date combinations were not explored for the cover-type analysis because actual species composition assumptions were not made for SAVI images prior to 1993. In other words, change was determined
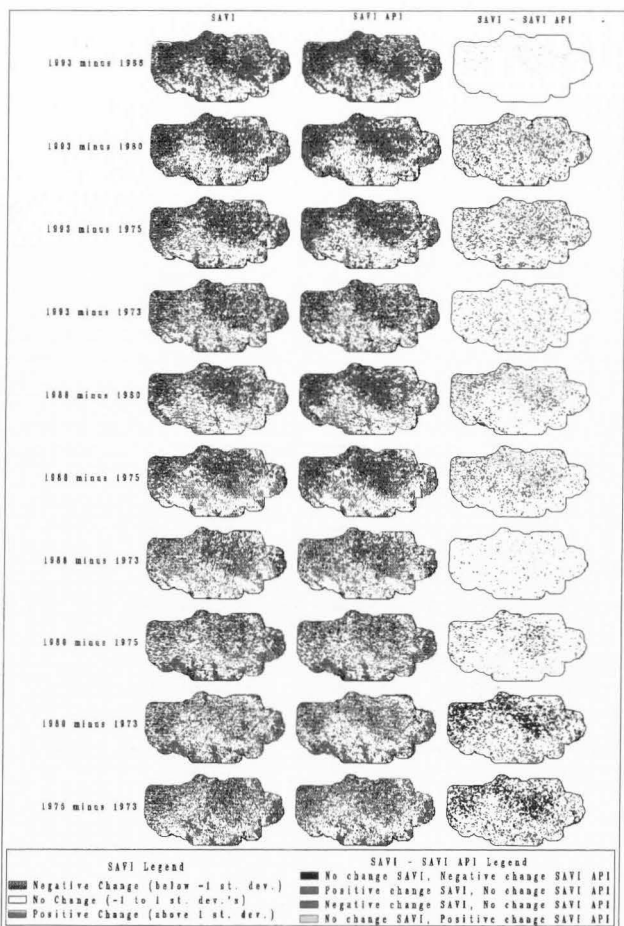
Fig. 17. SAVI API difference images were subtracted from SAVI image differences. Blue and yellow areas represent no change in SAVI, but negative and positive change in SAVI API, respectively. Green and red areas represent positive and negative change, respectively, in SAVI, but no change in SAVI API.

A. 1993 - 1988   B. 1993 - 1980

C. 1993 - 1975   D. 1993 - 1973

Legend
Negative Change (below -1 st. dev.)
No Change (-1 to 1 st. dev.'s)
Positive Change (above 1 st. dev.)

0 1 2 3 4 5
MILES
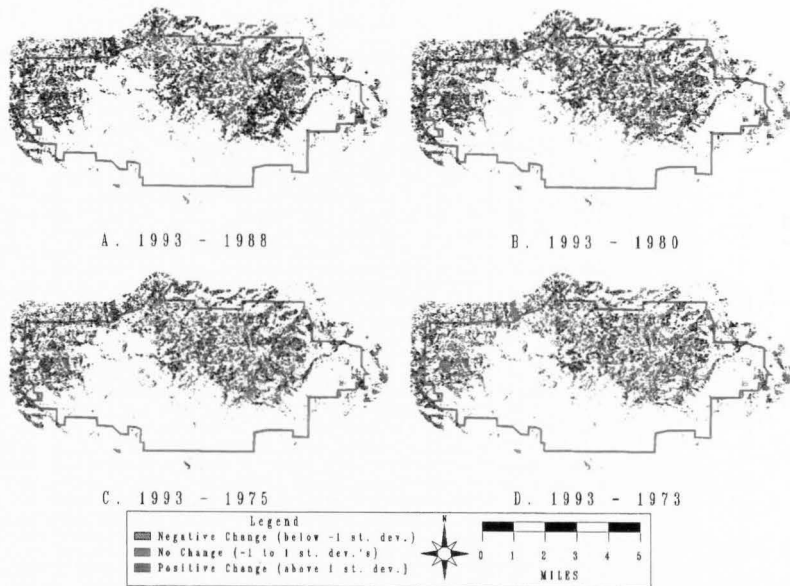
Fig. 18. Oakbrush cover-type difference images. Current (1993) oakbrush cover-type areas were compared to identical areas of previous years to determine areas of oakbrush that increased in SAVI, decreased in SAVI, and remained the same.

A. 1993 - 1988

B. 1993 - 1980

C. 1993 - 1975

D. 1993 - 1973

Legend

Negative Change (below -1 st. dev.)
No Change (-1 to 1 st. dev.'s)
Positive Change (above 1 st. dev.)

N

0 1 2 3 4 5
MILES
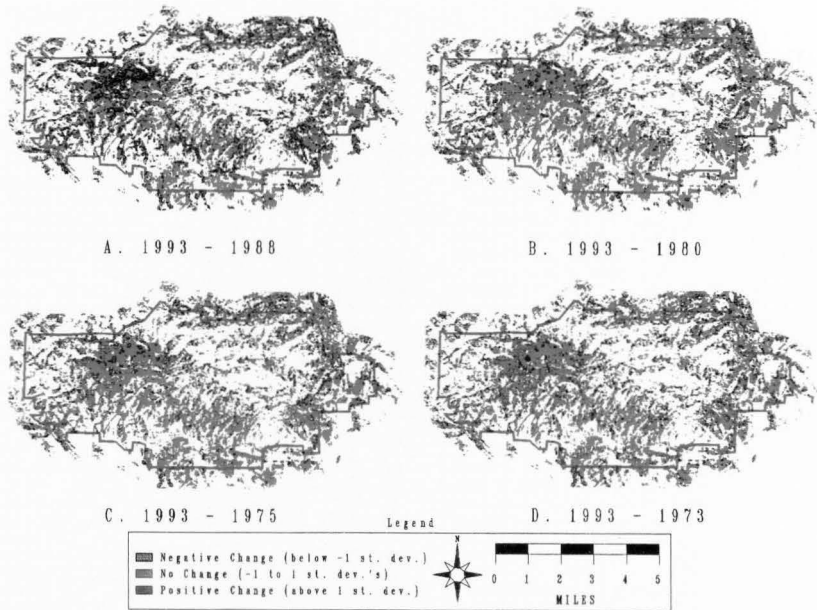
Fig. 19.   Sagebrush cover-type difference images. Current (1993) sagebrush cover-type polygons were compared to identical areas of previous years to determine amount of sagebrush that increased in SAVI, decreased in SAVI, and remained the same for that cover-type.

A. 1993 - 1988   B. 1993 - 1980

C. 1993 - 1975   D. 1993 - 1973

Legend

Negative Change (below -1 st. dev.)
No Change (-1 to 1 st. dev.'s)
Positive Change (above 1 st. dev.)

0   1   2   3   4   5
MILES
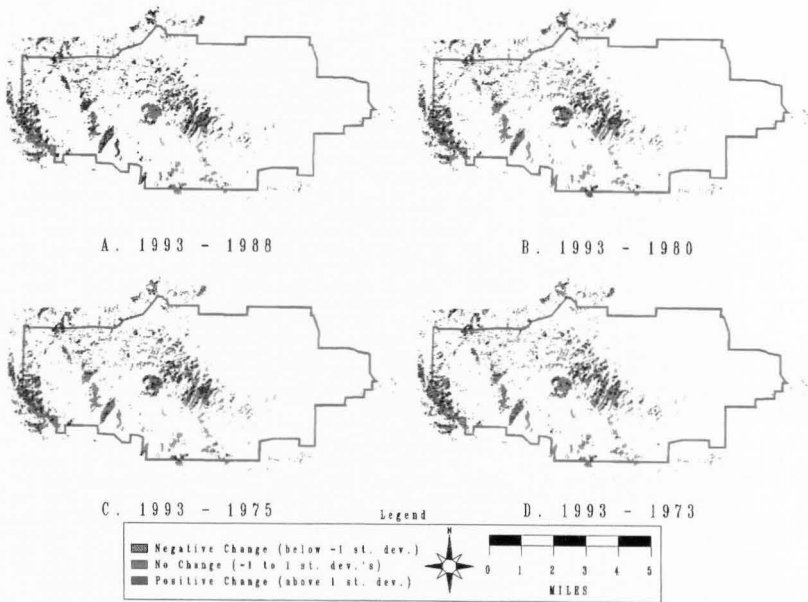
Fig. 20. Juniper cover-type difference images. Current (1993) juniper cover-type polygons were compared to identical areas of previous years to determine areas that increased in SAVI, decreased in SAVI, and remained the same for that cover-type.

A. 1993 - 1988   B. 1993 - 1980

C. 1993 - 1975   Legend   D. 1993 - 1973

Negative Change (below -1 st. dev.)
No Change (-1 to 1 st. dev.'s)
Positive Change (above 1 st. dev.)

0   1   2   3   4   5
MILES
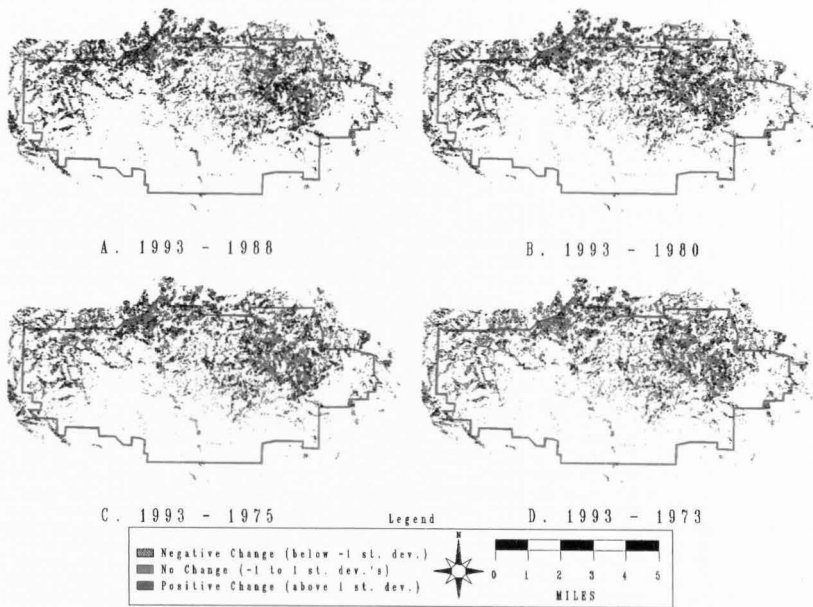
Fig. 21.   Oakbrush-sagebrush-grass mix cover-type difference images.   Current (1993) oakbrush-sagebrush-grass cover-type areas were compared to identical areas of previous years to determine areas that increased in SAVI, decreased in SAVI, and remained the same for that cover-type.

A. 1993 - 1988   B. 1993 - 1980

C. 1993 - 1975   Legend   D. 1993 - 1973

Negative Change (below -1 st. dev.)
No Change (-1 to 1 st. dev.'s)
Positive Change (above 1 st. dev.)

0   1   2   3   4   5
MILES
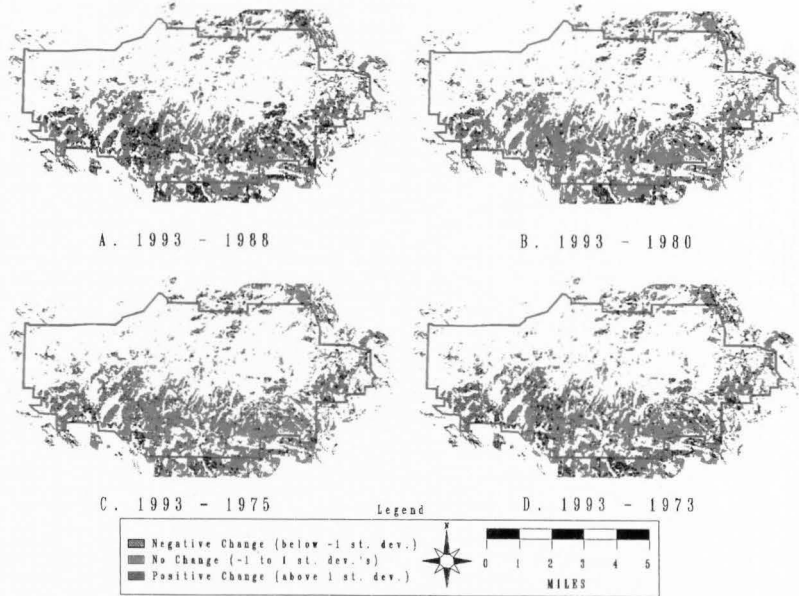
Fig. 22. Grass-sparse-shrub cover-type difference images. Current (1993) grass sparse shrub type polygons were compared to identical areas of previous years to determine areas that increased in SAVI, decreased in SAVI, and remained the same for that cover-type.

A. 1993 - 1988   B. 1993 - 1980

C. 1993 - 1975   Legend   D. 1993 - 1973

Legend
Negative Change (below -1 st. dev.)
No Change (-1 to 1 st. dev.'s)
Positive Change (above 1 st. dev.)

0 1 2 3 4 5
MILES
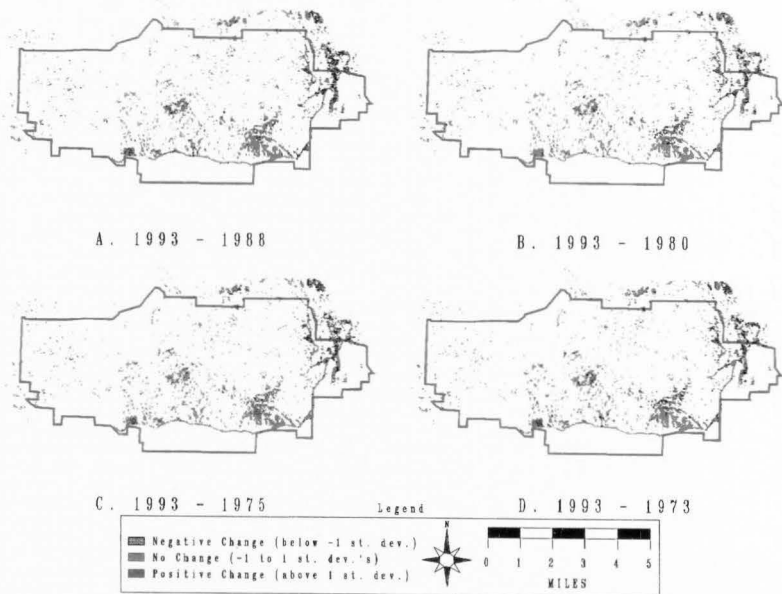
Fig. 23. Bare/annual weed cover-type difference images. Current (1993) bare/annual weed cover-type polygons were compared to identical areas that increased in SAVI, decreased in SAVI, and remained the same for that cover-type.

60

A. 1993 - 1988   B. 1993 - 1980

C. 1993 - 1975   D. 1993 - 1973

Legend

▨ Negative Change (below -1 st. dev.)
▦ No Change (-1 to 1 st. dev.'s)
▬ Positive Change (above 1 st. dev.)

0 1 2 3 4 5
MILES
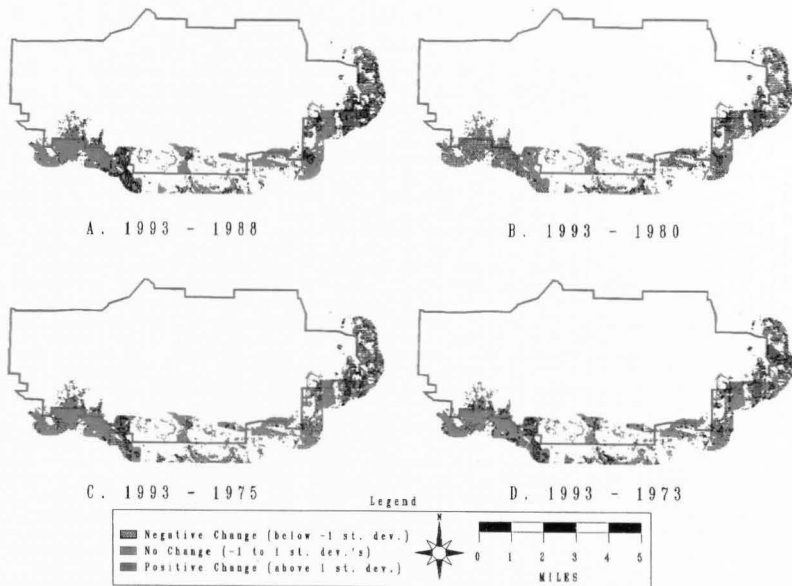
Fig. 24. Agriculture cover-type difference images. Current (1993) agriculture cover-type polygons were compared to identical areas of previous years to determine areas that increased in SAVI, decreased in SAVI, and remained the same for that cover-type.

from SAVI brightness values that are directly related to biomass. The change measures biomass, not composition. Since plant species composition is known only for the 1993 image, biomass change analysis of cover types (known composition) is only valid for image difference combinations including 1993.

**UNSUPERVISED CLASSIFICATION OF
SAVI COMPOSITE IMAGE**

A composite SAVI image of the five-period data set was generated with each of the channels containing a SAVI image for a different year in sequence. An unsupervised classification (ISODATA clustering algorithm) of this composite image produced sixteen spectral clusters. A maximum likelihood classification of the composite image generated a map of "trend" clusters (Figure 25).
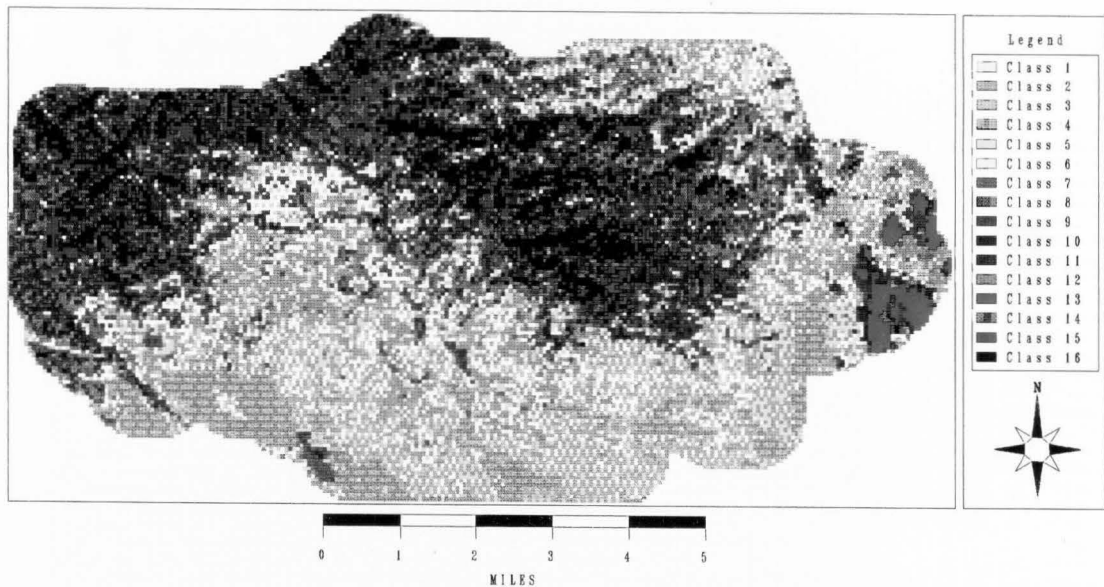
Fig. 25. Unsupervised classification of a composite image made up of five layers each consisting of a SAVI image from a different year. The classes or "trend types" reveal areas of similar trend for the time interval studied (1973-1993).

RESULTS

LAND USE/LAND COVER CLASSIFICATION

Ground truth data were collected in the summer of 1993
with a Trimble global positioning system (GPS). Eighty-two
data points served to test the accuracy of the
classification (Campbell, 1987). Overall map accuracy was
estimated at 89% (Table 3).

IMAGE DIFFERENCE APPROACH

Overall Difference

The image difference statistics for overall change are
summarized in Table 4. The overall trend is negative in all
difference image-year combinations except for the 1993 minus
1988 case. This shift is seen in Figure 26 where there is a
negative trend from 1973 to 1980, and a positive trend
between 1988 and 1993 for all years analyzed. Although a
positive trend was detected from 1988 to 1993, 1993 has a
negative trend when compared to every other year.
Inspection of Table 4 reveals the highest absolute change in
image combinations in which 1973 is subtracted from other

TABLE 3. OVERALL MAP ACCURACY OF LAND USE/LAND COVER
          CLASSIFICATION BASED ON GPS POINTS.

Classes	J	O	S	GSS	OSG	BAW	Accuracy
J	21	0	0	3	0	1	21/25 = 0.84
O	0	15	1	0	0	0	15/16 = 0.94
S	0	0	22	1	0	0	22/23 = 0.96
GSS	0	0	2	11	0	0	11/13 = 0.85
OSG	0	0	1	0	4	0	4/5 = 0.80
BAW	0	0	0	0	0	0	NA
Total	21	15	26	15	4	1	73/82 = 0.89

The classes on the left of the Table represent actual field
classes. The classes on the top of the Table represent map
classes. Land-cover classes were abbreviated (J = Juniper,
O = Oakbrush, S = Sagebrush, GSS = Grass-sparse-shrub, OSG =
oakbrush-sagebrush-grass, BAW = Bare/annual weed).

TABLE 4. OVERALL IMAGE DIFFERENCE STATISTICS. AREAS OF
NEGATIVE CHANGE, NO CHANGE, AND POSITIVE CHANGE WERE
QUANTIFIED. TREND WAS QUANTIFIED BY SUBTRACTING NEGATIVE
CHANGE FROM POSITIVE CHANGE. YEAR COMBINATIONS WITH
POSITIVE TREND REVEAL MORE POSITIVE CHANGE THAN NEGATIVE
CHANGE FOR THAT TIME PERIOD. YEAR COMBINATIONS WITH
NEGATIVE TREND REVEAL MORE NEGATIVE CHANGE THAN POSITIVE
CHANGE FOR THAT TIME PERIOD.

Years	Negative Change (ha.)	No Change (ha.)	Positive Change (ha.)	Trend (Pos-Neg) (ha.)
1993-1988	1369.440	16078.950	2655.810	+1286.370
1993-1980	2759.680	14775.680	2698.880	-60.800
1993-1975	3026.560	14529.920	2677.760	-348.800
1993-1973	3626.880	14582.399	2024.960	-1601.920
1988-1980	3489.920	14811.520	1932.800	-1557.120
1988-1975	3954.560	14457.600	1811.200	-2143.360
1988-1973	3809.920	15338.239	1086.080	-2723.840
1980-1975	3335.040	14769.920	2129.280	-1205.760
1980-1973	3570.560	15022.080	1641.600	-1928.960
1975-1973	3673.600	14917.120	1643.520	-2030.080
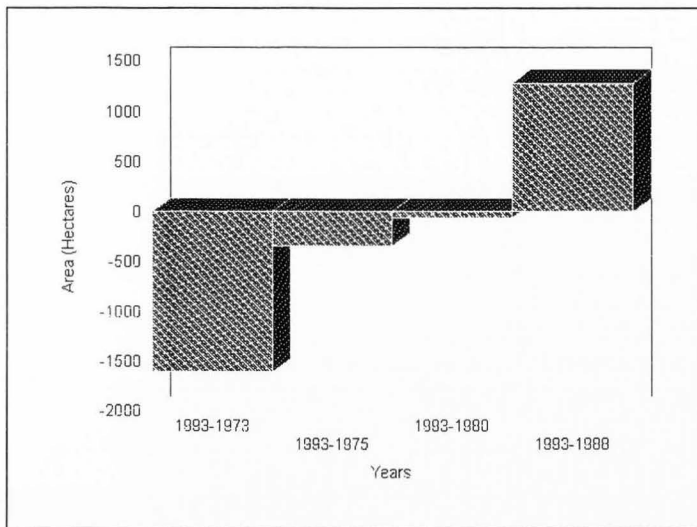
Fig. 26. Overall vegetation trend. Trend was calculated by subtracting negative change (hectares) from positive change (hectares) for all difference images including 1993. A negative trend was detected when 1993 was compared to 1973, 1975, and 1980 and a positive trend when 1993 was compared to 1988.

years. This shows that 1973 was the "greenest" of the

imagery of the selected 5 years. Since image difference

combinations including 1993 minus 1973, 1975, and 1980

reveal a negative trend and combinations including 1993

minus 1988 reveal a positive trend, 1988 is the least

"green" of the years. This vegetation trend matches the

climate trend. The earliest year received the most

precipitation and 1988 received the least of the years

studied.

The SAVI API difference images were noticeably

different from the SAVI difference images for several year

combinations (Figure 17 and Table 5). Image combinations

that had the most difference between SAVI image differences

calculated with an L = 0.5 and those calculated with L based

on API were 1993 minus 1980, 1993 minus 1975, 1988 minus

1980, 1988 minus 1975, 1980 minus 1973, and 1975 minus 1973.

These difference images were all "dry, wet" combinations;

one year has a low API value on satellite acquisition and

the other has a high API. Combinations of yellow and red or

blue and green are apparant (Figure 17). The yellow and red

combinations reveal a "downward" shift in change when SAVI

is compared to SAVI API; red areas were classified as no

change in SAVI API, but as negative change in SAVI, and

yellow areas were classified as positive change in SAVI API,

but as no change in SAVI (Figure 17). The blue and green

combination images reveal a relative "upward" shift in

change when SAVI is compared to SAVI API; blue areas were

TABLE 5. DIFFERENCE BETWEEN SAVI AND SAVI API. IDENTICAL
AREAS THAT WERE CLASSIFIED AS NO CHANGE IN SAVI DIFFERENCE
IMAGES, BUT AS NEGATIVE CHANGE AND POSITIVE CHANGE IN SAVE
API DIFFERENCE IMAGES ARE QUANTIFIED IN COLUMNS 2 AND 3,
RESPECTIVELY. AREAS THAT WERE CLASSIFIED AS POSITIVE AND
NEGATIVE IN SAVI IMAGE DIFFERENCES, BUT AS NO CHANGE IN SAVI
API ARE QUANTIFIED IN COLUMNS 4 AND 5, RESPECTIVELY. AREAS
THAT WERE CLASSIFIED THE SAME IN BOTH SAVI AND SAVI API ARE
REPRESENTED IN COLUMN 6.

Year	SAVI = No Change, SAVI API = Neg. Change (ha.)	SAVI = No Change, SAVI API = Pos. Change (ha.)	SAVI = Pos Change, SAVI API = No Change (ha.)	SAVI = Neg Change, SAVI API = No Change (ha.)	SAVI = SAVI API (ha.)
1993-1988	0.000	10.530	0.000	9.360	20084.311
1993-1980	2.970	529.470	206.190	752.040	18613.530
1993-1975	5.760	440.280	106.380	756.630	18795.151
1993-1973	0.000	18.990	32.490	307.440	19745.281
1988-1980	74.070	590.310	13.320	457.470	18969.031
1988-1975	16.920	434.160	9.360	578.340	19053.721
1988-1973	67.410	34.830	10.260	14.490	19977.210
1980-1975	177.120	17.730	155.520	24.480	19729.351
1980-1973	597.600	32.940	337.320	409.140	18727.200
1975-1973	556.110	16.290	452.970	267.570	18811.261

classified as negative change in SAVI API, but as no change
in SAVI; and green areas were classified as no change in
SAVI API, but as positive change in SAVI (Figure 17).
It seems as though most of the difference between SAVI and
SAVI API is located in the oakbrush cover type (Figures 9
and 17).

Cover-Type Difference

The image difference statistics for vegetation cover
class change are summarized in Table 6. The extreme case is
the bare/annual weed class, which has more negative than
positive change for all image differences. Every other
class reveals a dominant trend for three of the image
combinations followed or preceded by a shift in trend. The
sagebrush, grass-sparse-shrub, and agriculture classes all
have a negative trend (more negative change than positive
change) in image difference combinations that include 1973,
1975, and 1980. These grass and shrub dominated classes all
change polarity for the 1993-1988 case in which they all
have a positive trend (Figure 27).

TABLE 6. COVER-TYPE IMAGE DIFFERENCE STATISTICS. AREAS OF
NEGATIVE CHANGE, NO CHANGE, AND POSITIVE CHANGE WERE
QUANTIFIED.   TREND WAS QUANTIFIED BY SUBTRACTING NEGATIVE
CHANGE FROM POSITIVE CHANGE.

Cover	Years	Negative	No	Positive	Trend
O	1993-1988	266.22	1067.49	540.72	+274.50
O	1993-1980	248.04	1023.12	603.27	+355.23
O	1993-1975	297.81	976.59	600.03	+302.22
O	1993-1973	484.47	1008.63	381.33	-103.14
S	1993-1988	254.07	3102.03	548.10	+294.03
S	1993-1980	532.98	3017.70	353.52	-179.46
S	1993-1975	822.96	2783.79	297.45	-525.51
S	1993-1973	995.76	2616.03	292.41	-703.35
J	1993-1988	62.19	578.07	130.68	+68.49
J	1993-1980	90.63	503.46	176.85	+86.22
J	1993-1975	90.54	492.93	187.47	+96.93
J	1993-1973	151.92	489.24	129.78	-22.14
OSG	1993-1988	259.29	1066.50	448.11	+188.82
OSG	1993-1980	258.12	1046.88	468.90	+210.78
OSG	1993-1975	329.76	1011.51	432.63	+102.87
OSG	1993-1973	484.74	996.66	292.50	-192.24
GSS	1993-1988	105.30	2669.85	238.95	+133.65
GSS	1993-1980	370.89	2485.26	157.95	-212.94
GSS	1993-1975	657.63	2234.79	121.68	-535.95
GSS	1993-1973	619.74	2195.82	198.54	-421.20
AG	1993-1988	111.06	1283.49	269.19	+158.13
AG	1993-1980	784.08	726.12	153.54	-630.54
AG	1993-1975	372.15	1118.97	172.62	-199.53
AG	1993-1973	316.44	1087.38	259.92	-56.52
BAW	1993-1988	55.17	438.57	49.41	-5.76
BAW	1993-1980	101.34	397.44	44.37	-56.97
BAW	1993-1975	175.95	320.94	46.26	-129.69
BAW	1993-1973	137.43	347.22	58.50	-78.93

Land-cover classes were abbreviated (J = Juniper, O =
Oakbrush, S = Sagebrush, GSS = Grass-sparse-shrub, OSG =
Oakbrush-Sagebrush-Grass, AG = Agricultrure, and BAW =
Bare/annual weed).
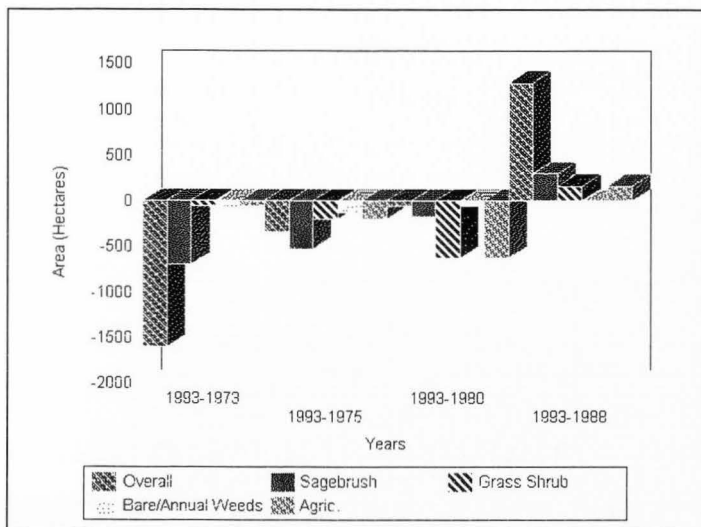
Fig. 27. Grass-and-shrub-dominated vegetation class trends.
Trend was calculated by subtracting negative change
(hectares) from positive change (hectares) for all grass and
shrub vegetation class difference images including 1993.

The tree- and brush-dominated classes reveal the

opposite pattern. Oakbrush, oakbrush-sagebrush-grass mix,

and juniper classes all reveal a negative trend for the

1993-1973 case, and a positive trend for the other year

combinations (those including 1975, 1980, and 1988) (Figure

28).
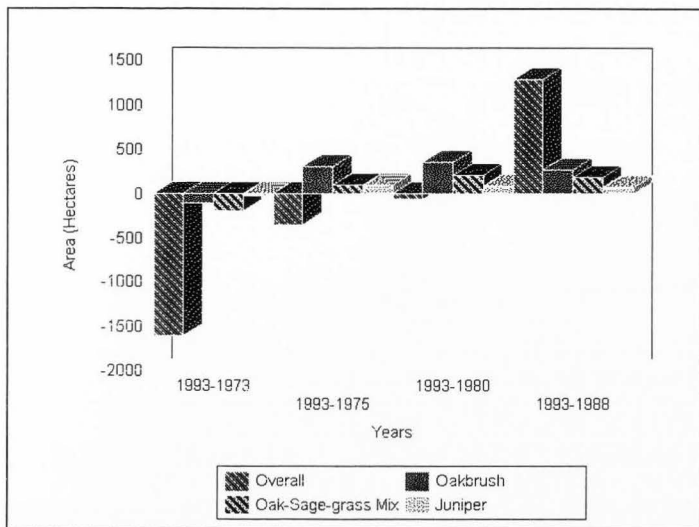
Fig. 28. Tree- and brush-dominated vegetation class trends. Trend was calculated by subtracting negative change (hectares) from positive change (hectares) for all tree and brush vegetation class difference images including 1993.

UNSUPERVISED CLASSIFICATION APPROACH

The spectral signatures for the sixteen trend classes (trend types) generated from the SAVI composite image are displayed in Figures 29-31. These signatures represent the trend over the last 20 years for each of the sixteen classes.
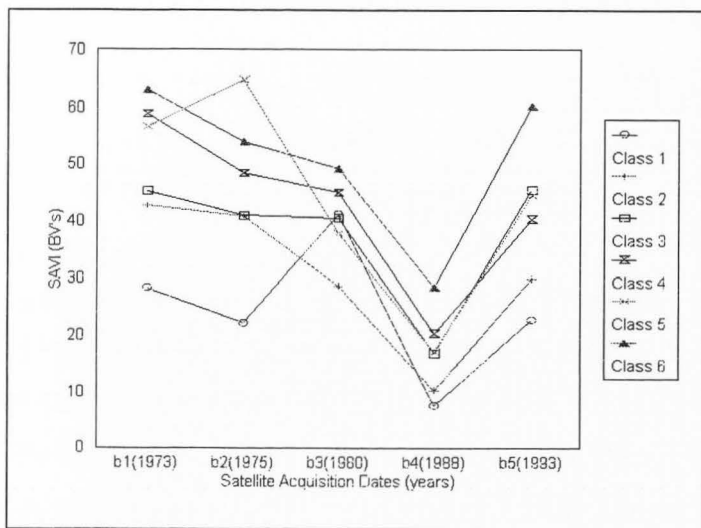
Fig. 29. SAVI composite trend type classes 1-6. Graph lines depict trend by revealing SAVI brightness values over the 20-year time interval between 1973 to 1993.
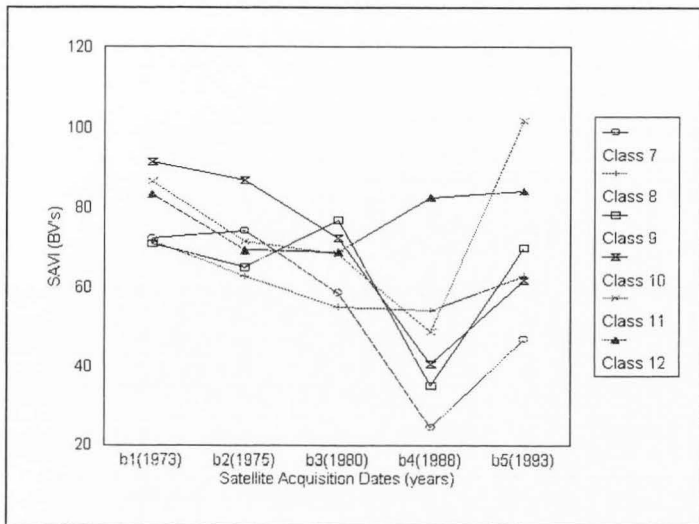
Fig. 30. SAVI composite trend type classes 7-12. Graph lines depict trend by revealing SAVI brightness values over the 20-year time interval between 1973 to 1993.
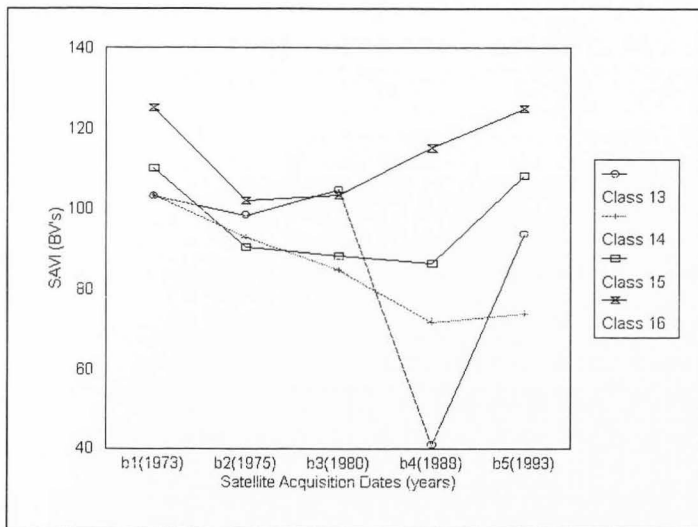
Fig. 31. SAVI composite trend type classes 13-16. Graph lines depict trend by revealing SAVI brightness values over the 20-year time interval between 1973 to 1993.

Summaries between these sixteen trend types and cover class, aspect, and slope are shown in Tables 7, 8, and 9, respectively. The trend types do not represent a particular cover class, but rather are associated with a variety of cover classes.

Trend types were separated based on similarity of spectral signatures to explain trend patterns. Trend types

TABLE 7. TREND TYPE CLASS BY LAND USE/LAND COVER TYPE.
TREND TYPE CLASSES WHICH WERE GENERATED FROM THE 5-YEAR DATA
SET (1973, 1975, 1980, 1988, 1993) WERE COMPARED TO CURRENT
(1993) LAND USE/LAND COVER CLASSES IN A GIS TO DETERMINE
COVER-TYPE ASSOCIATION. TREND TYPE CLASSES ARE DISPLAYED IN
THE FAR LEFT COLUMN WHILE COVER-TYPE CLASSES ARE DISPLAYED
ALONG THE TOP ROW. RESULTS ARE DISPLAYED IN PERCENTAGES
(PERCENT COVER CLASS MAKING UP TREND TYPE CLASS).

C	O	OSG	S	GSS	J	VAG	BAG	BAW	RIP	WAT	CL	CW
1	0.87	1.18	5.60	18.25	0.15	0.46	68.95	1.39	1.03	0.05	0.00	2.06
2	0.05	0.05	19.66	46.77	0.72	0.05	21.15	9.39	0.31	0.10	0.00	1.75
3	0.64	1.42	32.03	48.35	1.83	0.05	7.79	6.92	0.27	0.05	0.00	0.64
4	0.04	1.09	44.94	41.26	4.00	0.00	2.87	5.30	0.08	0.00	0.00	0.40
5	0.75	2.66	34.52	37.84	1.49	1.00	15.02	5.98	0.25	0.00	0.00	0.50
6	1.12	6.30	56.89	16.08	13.35	0.21	2.14	3.53	0.11	0.00	0.05	0.21
7	4.48	9.69	48.45	23.21	3.99	0.16	4.97	4.48	0.16	0.00	0.16	0.24
8	12.59	15.98	36.68	7.72	19.69	0.00	3.17	3.63	0.15	0.08	0.15	0.15
9	14.81	21.53	40.55	7.06	9.68	1.14	2.85	1.71	0.23	0.00	0.23	0.23
10	20.75	24.69	35.45	8.07	4.51	0.48	2.69	2.40	0.00	0.00	0.96	0.00
11	33.19	24.73	19.06	2.46	14.45	3.21	0.54	1.82	0.21	0.00	0.11	0.21
12	35.96	26.38	15.31	2.63	10.42	1.50	4.98	1.78	0.09	0.38	0.28	0.28
13	32.60	19.32	9.14	1.77	2.95	20.65	12.83	0.59	0.00	0.00	0.15	0.00
14	44.90	38.66	9.49	0.97	2.64	0.35	0.26	1.14	0.00	0.00	1.58	0.00
15	58.18	33.42	2.80	0.33	4.23	0.22	0.11	0.60	0.00	0.00	0.11	0.00
16	83.09	14.75	0.35	0.06	1.35	0.12	0.06	0.18	0.00	0.00	0.00	0.06

C = classes, J = juniper, O = oakbrush, S = sagebrush, GSS =
grass-sparse-shrub, OSG = oakbrush-sagebrush-grass, VAG =
vegetated agriculture, BAG = bare agriculture, RIP =
riparian, CL = cloud, CW = Camp Williams compound, WAT =
water, and BAW = Bare/annaul weed.

TABLE 8. TREND TYPE BY ASPECT. TREND TYPE CLASSES WERE COMPARED TO A DIGITAL ELEVATION MODEL (DEM) IN A GIS TO DETERMINE THEIR ASSOCIATION WITH ASPECT. TREND TYPE CLASSES ARE DISPLAYED IN THE FAR LEFT COLUMN WHILE ASPECT CLASSES ARE DISPLAYED ALONG THE TOP ROW. RESULTS ARE DISPLAYED IN PERCENTAGES (PERCENT OF ASPECT CLASS MAKING UP TREND TYPE CLASS).

Class	East	North-east	North	North-west	West	South-west	South	South-east	Flat
1	16.05	11.22	7.49	5.10	4.51	10.07	16.42	18.53	10.62
2	17.01	12.15	5.70	2.58	4.76	12.69	22.76	22.36	0.00
3	13.94	14.12	6.20	2.99	6.83	13.85	21.04	20.95	0.15
4	15.85	15.24	8.87	5.56	7.86	12.14	16.45	17.98	0.04
5	19.30	16.27	4.91	3.52	6.30	11.69	16.35	21.42	0.24
6	15.27	14.36	9.57	5.80	7.71	13.09	16.59	17.55	0.05
7	17.55	12.89	4.98	3.24	7.35	10.91	20.88	22.21	0.00
8	18.62	17.11	8.10	4.62	9.08	12.11	15.90	15.14	0.23
9	12.37	11.15	8.25	6.35	7.92	15.38	21.40	17.06	0.11
10	16.18	13.66	8.23	5.99	6.92	10.66	15.52	22.73	0.09
11	11.79	17.64	13.13	12.72	16.10	11.69	9.65	7.28	0.00
12	13.75	20.67	12.75	9.65	10.84	10.75	10.75	10.66	0.18
13	14.71	14.29	8.91	9.76	10.75	11.46	15.55	13.72	0.85
14	22.28	16.67	7.14	6.04	6.46	8.33	14.80	18.28	0.00
15	15.96	22.84	15.85	13.02	10.51	6.19	6.67	8.96	0.00
16	12.41	29.31	26.67	16.90	5.11	2.24	1.96	4.94	0.46

TABLE 9.   TREND TYPE CLASS BY SLOPE.   TREND TYPE CLASSES
WERE COMPARED TO A DIGITAL ELEVATION MODEL (DEM) IN A GIS TO
DETERMINE THEIR ASSOCIATION WITH SLOPE.   TREND TYPE CLASSES
ARE DISPLAYED IN THE FAR LEFT COLUMN WHILE SLOPE CLASSES ARE
DISPLAYED ALONG THE TOP ROW (IN DEGREES).   RESULTS ARE
DISPLAYED IN PERCENTAGES (PERCENT OF SLOPE CLASS MAKING UP
TREND TYPE CLASS).

Class	1-5	6-10	11-15	16-20	21-25	26-30	31-35	36-40	41-45	46-50
1	54.37	26.81	17.70	0.75	0.28	0.05	0.00	0.05	0.00	0.00
2	39.71	29.42	16.98	9.19	3.15	1.20	0.35	0.00	0.00	0.00
3	35.40	34.17	15.54	11.12	3.33	0.36	0.05	0.00	0.05	0.00
4	29.44	37.40	19.49	8.57	4.12	0.85	0.08	0.00	0.00	0.04
5	38.56	26.26	15.94	12.30	5.20	1.57	0.17	0.00	0.00	0.00
6	26.07	36.54	19.28	11.65	4.97	1.44	0.05	0.00	0.00	0.00
7	24.48	26.31	19.08	14.07	12.64	3.10	0.24	0.08	0.00	0.00
8	16.50	33.38	22.41	16.35	9.29	1.84	0.23	0.00	0.00	0.00
9	23.60	29.21	16.97	16.63	10.45	2.92	0.11	0.00	0.11	0.00
10	15.44	24.01	23.73	19.21	13.56	3.95	0.09	0.00	0.00	0.00
11	14.35	24.22	24.95	17.88	11.75	6.03	0.83	0.00	0.00	0.00
12	20.06	28.70	22.82	13.89	10.67	3.40	0.46	0.00	0.00	0.00
13	39.50	13.95	19.09	14.10	9.54	3.52	0.29	0.00	0.00	0.00
14	8.57	25.28	25.71	20.91	14.40	4.46	0.69	0.00	0.00	0.00
15	6.93	23.32	28.35	23.27	11.96	4.98	1.19	0.00	0.00	0.00
16	5.16	18.42	26.94	24.91	17.73	5.91	0.93	0.00	0.00	0.00

2, 3, 4, 6, and 10 are displayed in Figure 32. These types

represent the most common pattern of trend--gently

decreasing from 1973 to 1980 followed by a large decrease in

1988 and increase in 1993. Trend types 2, 3, 4, and 6 are
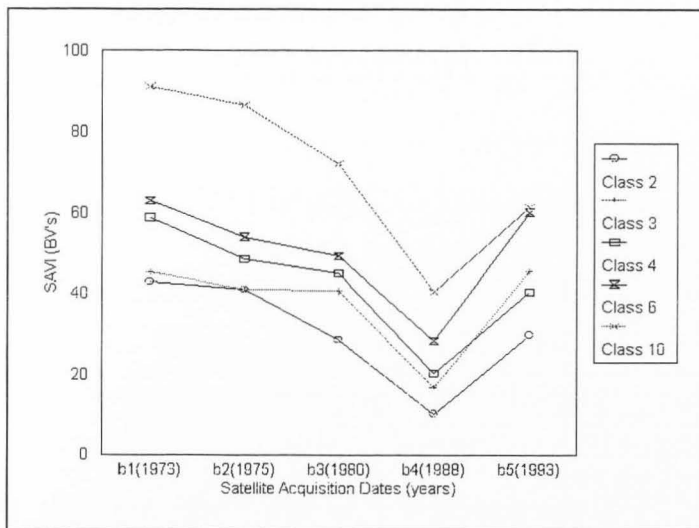
Fig. 32. Trend pattern one (trend types 2, 3, 4, 6, and 10). Trend types were combined because of similarity of shape. These trend types follow the precipitation pattern.

associated with shrub and grass dominated classes (sagebrush, grass-sparse shrub, and agriculture). They are associated mostly with gentle southern- and eastern-facing slopes. Trend type 10 is associated with oakbrush and sagebrush on southeastern gentle to moderately steep slopes.

Trend types 5, 7, 11, and 13 were all very similar to the previous trend types (Figure 33). However, their trend patterns were different. Trend types 5 and 7 both increased slightly from 1973 to 1975 and then dropped quite steeply from 1975 to 1980 and 1980 to 1988. They both increased again from 1988 to 1993. Type 11 was very similar except that from 1988 to 1993, it experienced an increase (approximately 55 BV's) to a level above its origin (1973). Type 13 is different because it experienced an extraordinary decrease in 1988 (about 60 BV's) followed by a large increase in 1993 (about 50 BV's).

Trend types 5 and 7 are associated with sagebrush and grass-sparse shrub classes, which are also associated with gentle southeastern slopes. Type 11 is associated with oakbrush, sagebrush, and juniper classes on gentle to moderate slopes. Type 11 also has a weak association to northern aspects. Type 13 is associated with oakbrush, oakbrush-sagebrush mix, and agriculture classes on gentle eastern slopes.

Trend types 1, 9, and 14 are different from all others (Figure 34). Types 1 and 9 reveal an uncharacteristic peak
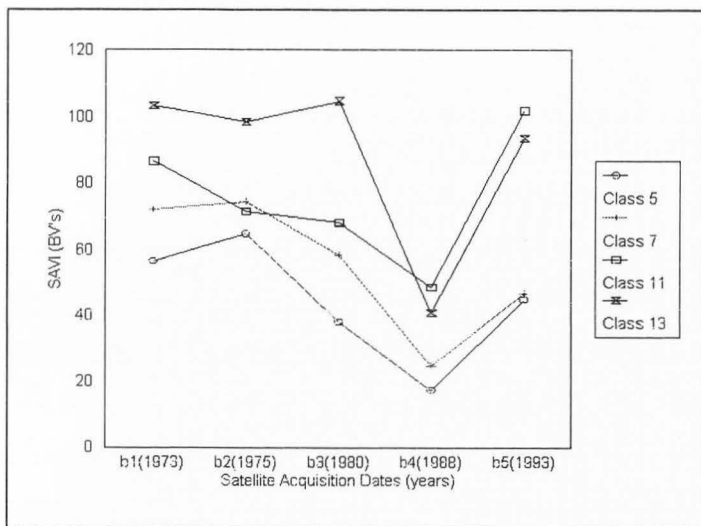
Fig. 33. Trend pattern two (trend types 5, 7, 11, and 13).
Trend types were combined because of similarity of shape.
These trend types all differ from the precipitation pattern.
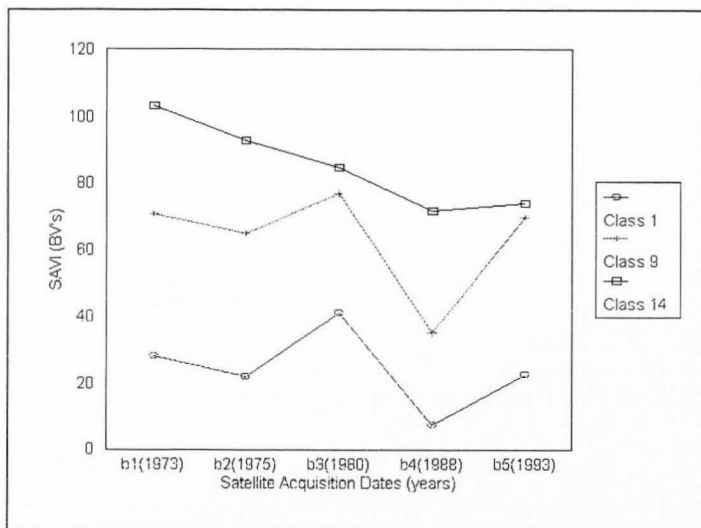
Fig. 34. Trend pattern three (trend types 1, 9, and 14). These types have uncharacteristic trends when compared to the others. Trend types 1 and 9 peak in 1980 while trend type 14 reveals an almost steady decline.

in 1980, while type 14 showed an almost steady decrease for all years studied. Type 1 is associated with agriculture on gentle southern and eastern slopes. Trend type 9 is dominated by sagebrush, oakbrush sagebrush mix, and oakbrush, gentle slopes, and southern aspects. Trend type 14 is characterized by oakbrush and oakbrush sagebrush mix cover classes, moderate to high slopes, and eastern aspects.

Trend types 8, 12, 15, and 16 are roughly represented
by U-shaped curves (Figure 35); none have the characteristic
large decrease from 1980 to 1988. In fact, two types (trend
types 12 and 16) actually increase from 1980 to 1988. Types
8 and 12 are associated with oakbrush, oakbrush-sagebrush-
grass mix, and sagebrush cover classes on moderate to steep
slopes. Type 8 is dominated by sagebrush and southeastern
slopes while class 12 is dominated by oakbrush with a weak
association to northeastern aspects. Types 15 and 16 are
associated with oakbrush on moderate to steep north-facing
slopes.

ANTECEDENT PRECIPITATION INDEX

The API values were quantified and displayed in Table
10. Soil moisture available from the beginning of the water
year (October 1) through satellite acquisition dates for
1973, 1975, 1980, 1988, and 1993 is displayed. The soil
moisture (API) was also totaled by month starting in March
and ending in the month of acquisition to depict soil
moisture drawdown during the growing seasons. These soil
moisture measurement differences, along with other
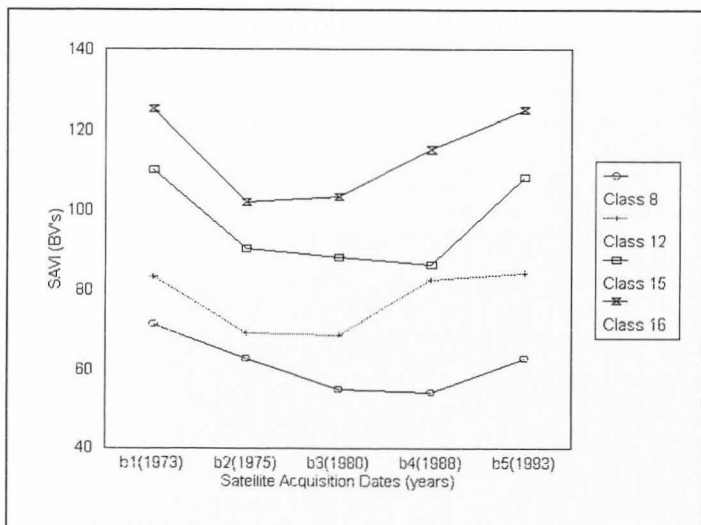
Fig. 35. Trend pattern four (trend types 8, 12, 15, and 16). These trend types were combined because they all display a general U-shaped pattern. These types might reveal areas that are less affected by precipiation changes.

TABLE 10. ANTECEDENT PRECIPITATION INDEX INFORMATION. SOIL
MOISTURE (MM) WAS QUANTIFIED TO DEPICT MOISTURE AVAILABILITY
FOR THE WATER YEAR (OCTOBER 1 THROUGH SATELLITE ACQUISITION)
AND DURING THE GROWING SEASONS AT CAMP WILLIAMS, UTAH.

Year	1973	1975	1980	1988	1993
Water Year	180.59	194.69	159.23	62.66	168.71
March	115.91	112.62	83.64	32.71	82.59
April	22.68	24.43	15.29	8.21	18.99
May	19.73	24.75	35.05	11.33	31.02
June	11.28	22.09	11.95	6.66	24.71
July	NA	NA	5.49	0.37	2.24
August	NA	NA	NA	1.34	NA

environmental variables, influence vegetation growth (Dugas,
1980).

DISCUSSION

IMAGE DIFFERENCE APPROACH

Overall Difference

Although a considerable difference was detected when SAVI API image combinations were compared to SAVI image combinations, it is unknown which is more representative of actual vegetation change. It may be that the SAVI API is better since it is based on soil moisture information. However, actual ground truthing is necessary to verify this hypothesis. A single adjustment factor for the entire image is the first step in a moisture standardized index, but is probably insufficient for realistic representation. This adjustment probably improves vegetation measurement for pixels with significant soil background, but may degrade vegetation measurement for pixels of no soil or little soil background (like oakbrush, where a great deal of difference was detected). A model should be developed and tested that considers soil moisture as well as vegetation cover (or percent bare ground) on a pixel-by-pixel basis. Because of the unknown relationship between actual vegetation

characteristics and VI differences due to API-based SAVI, SAVI difference images used for analysis were calculated with a constant L = 0.5.

These SAVI differences revealed lower BV's in 1993 than in 1973, 1975, and 1980, but higher than 1988. This means that there was a negative trend from 1973 to 1988 and a positive trend from 1988 to 1993. Even though the 1988 to 1993 interval has a positive trend, 1993 still has a negative trend when compared to every other year. This indicates that there was an overall negative change from 1973 to 1993 (20-year interval).

Four image difference intervals have been identified for in-depth examination because they are critical time periods for vegetation trend analysis at Camp Williams. They are (1) between 1988 and 1993, (2) between 1973 and 1993, (3) between 1973 and 1988, and (4) between 1973 and 1975. The first was identified because a shift from negative to positive trend occurred, the second because it represents the largest time interval available, the third because it represents the most change (largest absolute value of trend) of any difference image combination, and the

fourth because a large extent of change was identified for a short time period.

The shift from negative to positive trend during 1988 to 1993 is probably due at least in part to precipitation and fire disturbances. Inspection of precipitation data identified a shift from low to higher precipitation between 1988 and 1993. This difference was also shown in the soil moisture measurements (API). The year 1988 had low moisture during the critical growing season and prior to satellite acquisition, whereas 1993 had much more moisture available during the growing season (Figures 11 and 14). These differences in soil moisture can greatly influence vegetation development (Dugas, 1980).

Fire history of the camp also reveals at least two fires that burned approximately 814 hectares in 1987. Figure 36 clearly shows positive change within these fire boundaries. This indicates that fire recovery probably accounts for some of the positive trend between 1988 and 1993 for the entire camp. The low precipitation and fire disturbances probably account for low SAVI measurements in 1988, while the higher precipitation and vegetation recovery
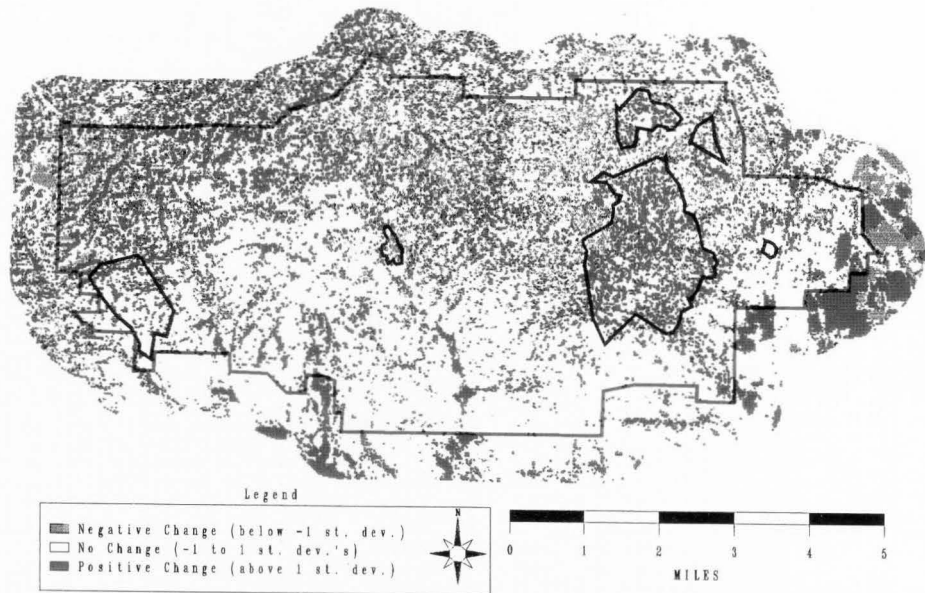
Fig. 36. 1993 minus 1988 SAVI difference image. Black lines depict fire boundaries. Green areas reveal an increase in SAVI in 1993, brown areas reveal a decrease in SAVI in 1993, and white areas reveal no change in SAVI between dates.

most likely account for higher SAVI values in 1993. This could then explain the shift from negative to positive trend during this time period.

The change from 1973 to 1993 represents a 20-year change and the longest time interval for the data available. This reveals a negative trend, where there is more area of negative change than positive change in 1993 compared to 1973. This shows a general decrease in vegetation characteristics measurable from SAVI (e.g., biomass) that could be directly related to both fire and precipitation. More precipitation was received during 1973 than 1993, which might explain the higher SAVI values in 1973.

The API also reveals very different soil moisture availability throughout the growing season for 1993 compared to 1973 (Figures 11 and 17 and Table 10). As shown in Table 10, 1973 had a great deal more soil moisture available early in the growing season (March and April) than 1993, but 1993 had much more available late in the growing season (May and June). These soil moisture differences can affect development of vegetation (Dugas, 1980). The 1973 soil moisture pattern had more water available during forb

development, which might significantly increase forb biomass (Figure 2). The 1993 soil moisture pattern had less moisture available early, but more later in the growing season, which might significantly increase grass and shrub biomass (Figure 2). This might explain part of the vegetation pattern seen for this time period. Also, in 1993, the two 1987 fires had not fully recovered (Godfrey, 1995), maybe accounting for less biomass and therefore lower SAVI values.

The time period between 1973 and 1988 represents the most change between any year combinations of difference images. This could also be partly explained by both precipitation and fire history. The most precipitation was experienced during 1973 while 1988 received the least. This likely resulted in more biomass in 1973 than in 1988. The API measurements similarly reveal a great deal more soil moisture in 1973 than in 1988 (Table 10). The two 1987 fires would also decrease biomass in 1988 when compared to 1973. The SAVI image difference associated with these fires is displayed in Figure 37. The likely decrease in biomass probably resulted in negative trend (brown areas) inside
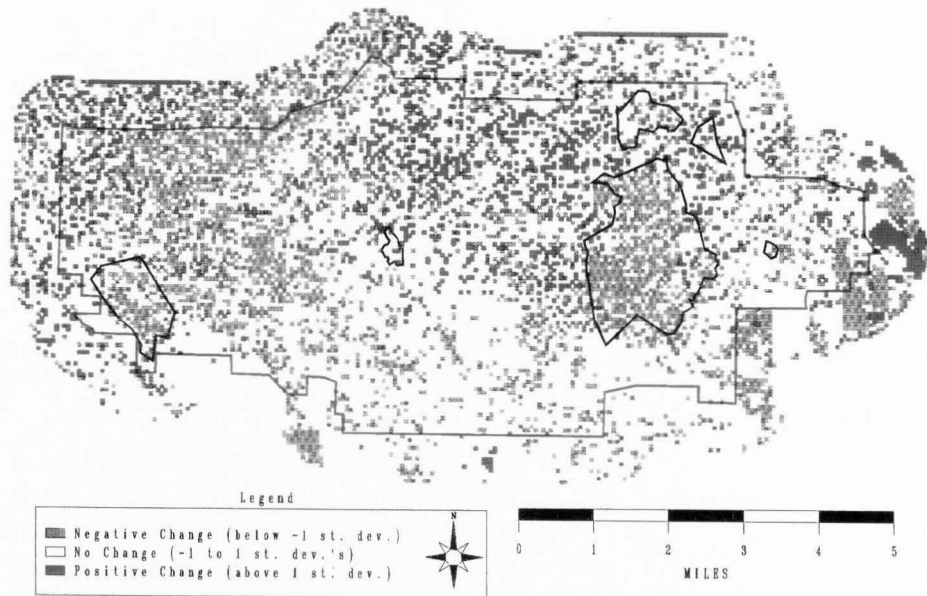
Fig. 37. 1988 minus 1973 SAVI difference image. Black lines depict fire boundaries.
Green areas reveal an increase in SAVI in 1988, brown areas reveal a decrease in SAVI
in 1988, and white areas reveal no change in SAVI between dates.

1987 fire polygons. The area of negative trend outside fire polygons is more likely related to precipitation changes.

The combination of low precipitation and fire disturbance in 1988 probably resulted in this year having the least amount of biomass (measured from SAVI). When this year was compared to the year with likely the most biomass (1973), it resulted in the largest amount of change (largest absolute value of trend).

The amount of absolute change detected for the 2-year time period between 1973 and 1975 was the third highest of all difference image combinations. The two image combinations that had more change both included 1988. This means that the 1975 minus 1973 case contained the largest amount of change for difference image combinations not including the driest year (1988). This reveals an unexpected result.

Inspection of precipitation data reveals almost no difference between 1973 and 1975. Water year and growing season soil moisture differences (Figure 11 and 12 and Table 10) provide more information; 1975 had more soil moisture in both May and June than did 1973. However, this does not

seem to support the large negative trend between these years either. The fire history data set also fails to explain this change.

Although this change is not explained, a time frame has been identified in which land and military management practices, disturbance history, and other physical influences need to be studied further. If the reasons for the vegetation change response measured during this time period are ever identified, current and historical knowledge would increase and better management plans could be developed.

Cover-Type Difference

Two time periods were identified as critical at Camp Williams for cover-type vegetation trend analysis. They are (1) between 1988 and 1993, and (2) between 1973 and 1975. These time periods were identified because of trend polarity shifts. The first interval seems to be critical in grass and shrub cover classes (sagebrush, grass sparse shrub, and agriculture; Figure 27), while the second is critical for

tree- and brush-dominated classes (oakbrush, oakbrush-
sagebrush-grass mix, and juniper; Figure 28).

Since cover-type change was determined using only
combinations including 1993, cover-type trend includes a
certain bias; more change would be expected in difference
image combinations comparing years over a greater time
period (e.g., 1993-1973) than over a shorter time period
(e.g., 1993-1988) unless outside influences (e.g., climate,
land-use, disturbance) affect the trend.

The bare/annual weed class is the only class that does
not switch polarity of trend. It remains negative for all
year combinations. The expected pattern of greater absolute
change as the time period for change detection increases is
seen with the exception of the time interval 1975 to 1993.
There was more absolute change during this time interval
than from 1973 to 1993. Since the bare/annual weed class is
mostly nonvegetated areas like roads or military activity
centers, a change in land use could explain the increase in
absolute difference in 1975. Construction of roads,
military ranges, or other land-use alterations may be the
cause for the difference.

The climatic influence of extremely low precipitation
(1988) is probably seen in the shrub-and-grass-dominated
classes (sagebrush, grass sparse shrub, and agriculture).
For each of these classes, there is a negative trend for all
image combinations except 1993 minus 1988. The positive
trend from 1988 to 1993 is correlated with precipitation.
Low precipitation in 1988 probably resulted in low SAVI
(biomass) values. High precipitation in 1993 likely
resulted in high SAVI values. Therefore, there is a
positive trend when 1988 is compared to 1993.

The tree-and brush-dominated classes reveal positive
trends for all year combinations except 1993 minus 1973.
Since there is a polarity shift of vegetation trend after
this time period (positive trend for 1993 minus 1975, 1993
minus 1980, and 1993 minus 1988), 1973 to 1975 marks an
important time period for identifying change in oakbrush and
juniper. This change does not seem to be related to fire
disturbance, but may be explained by precipitation data.
The only year studied that received more precipitation than
1993 was 1973. This might explain the negative trend when
1973 is subtracted from 1993. The other years (1975, 1980,

and 1988) all received less precipitation than 1993 and a
positive trend was revealed when they were subtracted from
1993. This pattern, then, might appear to follow
precipitation.

However, the response of the tree- and brush-dominated
classes is not sufficiently described by precipitation.
There is no solid explaination for the large difference
between 1973 to 1975. The precipitation difference between
these years was small (Figure 3), yet there was a shift in
trend polarity (Table 6). And, the vegetation difference
for the year combination with greatest precipitation
difference was less than years with smaller precipitation
differences; 1993 minus 1980 image difference combinations
for oakbrush, oakbrush-sagebrush-grass mix, and juniper were
all more positive than 1993 minus 1988 combinations. This
is opposite of what was expected; 1980 received about 406 mm
(16 inches) of precipitation while 1988 received about 152
mm (6 inches). The expected result would be more positive
change from 1988 to 1993 if vegetation change for these
classes follows precipitation. Figure 36 shows a positive
trend from 1988 to 1993, probably due to fire disturbance;

814 hectares of mostly oakbrush were burned in 1987. This should make the trend from 1988 to 1993 even more positive.

The interactions between vegetation, soil, climate, topography, and land-use and disturbance are complex and variable and therfore hard to understand. Precipitation and soil moisture variability, especially during the growing season (and just prior to image capture), could affect various types of vegetation differently (Table 10). This might provide a clue as to why certain results occurred. However, the generality of the soil moisture model and the lack of specific phenological data for Camp Williams limit the degree of explanation. Although change in the tree-dominated classes was detected for this time period, causation cannot be defined with any amount of certainty because of the limitations of the data and the stochastic nature of the environment. This time interval was also identified in the overall image difference approach as critical, but was not explained there either. These areas need to be studied further in an attempt to explain this pattern.

It does not appear that the critical time period in shrub and grass classes (1988 to 1993) is critical for tree-dominated classes; the trend decreases slightly from 1988 to 1993 for oakbrush, oakbrush-sagebrush-grass, and juniper when compared to the time period from 1980 to 1993. This shows that the large increase in trend from 1988 to 1993 seen in the shrub and grass classes is not seen in the tree and brush classes. The reason for this is unknown. Growing season precipitation and soil moisture variablility might be part of the explaination, but there are too many variables and not enough information to know for sure.

Likewise, it does not appear that the critical time period for the tree and brush classes (1973 to 1975) is critical for the shrub and grass classes as there is no obvious pattern nor dramatic change for this time period. The reason for this is also unknown. Since the cause of change in tree-dominated classes from 1973 to 1975 is not known, it is impossible to know why the shrub and grass classes were not affected by the same phenomena.

The same two time periods that were identified as critical for cover-type trend analysis (1988 to 1993 and

1973 to 1975) were also identified as critical for the

overall trend analysis. However, the cover-type analysis

was able to provide more information for these time periods

by distinguishing them as important for certain cover types.

The 1988 to 1993 interval seemed to be critical for shrub-

and-grass-dominated classes, and the 1973 to 1975 time

interval seemed to be critical for tree-dominated classes.

UNSUPERVISED CLASSIFICATION APPROACH

It would seem that the differences in trend are mostly

caused by precipitation and slope effect. Some trend

patterns are also directly related to fire disturbance and

land use. The most common pattern of trend is revealed in

trend types 2, 3, 4, 6, and 10. These types basically

follow the precipitation pattern over Camp Williams; a

decrease in precipitation results in a decrease in biomass,

and an increase in precipitation results in an increase in

biomass measured from SAVI.

The likely precipitation-driven patterns of these five

trend types is supported by the fact that they are all

associated with south-facing slopes. These slopes receive

more direct exposure to solar insolation and, therefore,

maintain less soil moisture for vegetation due to higher

evaporation. The vegetation on these slopes should then be

more sensitive to changes in precipitation.

Trend types 5, 7, 11, and 13 are all similar to the

previous assumed precipitation-driven trend types, but all

possess an attribute that cannot be explained by

precipitation alone. Trend types 5 and 7 increase in SAVI

values from 1973 to 1975 and have a rather steep decrease in

SAVI values from 1975 to 1980. This does not follow the

precipitation pattern, and cause for these trends is unknown

since fire disturbance and slope effects do not help explain

the pattern either.

Type 11 is unique because its SAVI values peak in 1993

after a low in 1988. This cannot be explained solely by

precipitation either, since 1993 received less precipitation

than 1973, yet 1993 reveals more biomass than 1973 for this

trend type. Fire disturbance may explain this pattern, in

part, since trend type 11 is partly contained within the

boundaries of a 1987 fire. However, its rather mild

decrease from 1980 to 1988 and its dramatic increase from

1988 to 1993 are somewhat a mystery. What attribute or combination of attributes (possibly cover type, slope, and aspect) that make trend type 11's increase between 1988 and 1993 different from the others is unknown.

Trend type 13 shows about the same amount of increase between 1988 and 1993 as trend type 11, but was preceeded by a decrease between 1980 and 1988. This is readily explained by its geographic location within Camp Williams. Trend type 13 is associated with oakbrush classes within the 1987 fire boundaries, and agricultural fields. It represents an oakbrush class that lost a great deal of biomass due to a fire disturbance in 1987, and almost fully recovered its biomass by 1993. This type is also associated with certain agricultural fields that were probably vegetated in every year except 1988.

Trend types 1, 9, and 14, also cannot be explained by correlation with precipitation alone. Types 1 and 9 both reach their highest SAVI values in 1980. Trend type 1 is associated with agriculture and, therefore, its peak in 1980 can be explained by differences in farming practices in that year. Trend type 9, however, is associated with sagebrush,

oakbrush, and oakbrush-sagebrush-grass cover classes. There
is no apparent explanation for this pattern found in the
fire or precipitation history. However, inspection of cover
type trend statistics (Table 6) confirms that for sagebrush,
oakbrush, and oakbrush-sagebrush-grass classes, there is
more positive change for the 1993 minus 1980 case than for
both the 1993 minus 1975 and 1993 minus 1988 cases. This
shows that the same peak in sagebrush and oakbrush classes
was found using both approaches to land cover dynamics.

Type 14 represents a class that has lost biomass for
every time interval studied except 1988 to 1993, in which it
remained about the same. This type was apparently not
particularly sensitive to precipitation, and may be
indicative of an oakbrush class degrading because of age or
unknown influences.

Trend types 8, 12, 15, and 16 are characterized very
generally by a U-shaped curve. These classes seem to be
more stable and are apparently less affected by
precipitation. This is clearly demonstrated by the 1980 to
1988 interval where no class experiences a dramatic drop in
biomass. In fact, trend classes 12 and 16 increase during

this time period. Although aspect may account for part of this increase, definite cause(s) is unknown and, therefore, further study of these areas is justified.

Types 12, 15, and 16 are all associated with northern exposures, but this is not the sole explanation for the increase from 1980 to 1988. This is apparent because type 12 has the weakest association with aspect and type 16 has the strongest, yet both show about the same increase. While type 16 continues to increase, type 12 remains the same for 1993. This does not necessarily mean that north-facing slopes will increase in biomass during drought years because type 15 did not. However, these north-facing slopes showed no significant decrease during the drought years.

This is directly related to the fact that north-facing slopes receive less direct sunlight and therefore remain cooler and more moist. This would favor vegetation during dry years and is seen in the stability of these four trend types.

All four U-shaped trend types have an association with the oakbrush cover type. As the trend-type numbers increase, so does their association with oakbrush (trend

type 8 has the least association with oakbrush while type 16

has the highest). As trend-type association with oakbrush

increases, its slope between 1973 and 1975 becomes more

negatively steep. This supports the findings in both the

overall and cover-type trend analysis of approach 1 that

1973 to 1975 is a critical time period for oakbrush.

CONCLUSIONS

There is no single factor that controls vegetation, but rather a combination of variables, including natural variability, and historical land use and disturbance (Gleason, 1926; Webb et al., 1970). The vegetation trends at Camp Williams, therefore, are not solely explained by precipitation. However, years of high precipitation are correlated with higher VI measurements, and thus trend analysis is influenced. Precipitation interactions with vegetation are highly complex and variable, and site specific (Dugas, 1980). Therefore, overall precipitation and soil moisture at and prior to satellite acquisition dates both reveal different and valuable information about vegetation characteristics. The precipitation and soil moisture patterns, especially during the growing season (Dugas, 1980) and most likely just prior to image capture, can greatly influence vegetation measurements from satellite imagery. These precipitation variables can help explain, partly, differences in SAVI values.

Vegetation trend at Camp Williams has also been found to be influenced by variables other than precipitation. It

was shown that fire disturbance and land-use (agriculture) changes are also detectable using this approach.

Vegetation trend analysis and results are applicable only to years in which images were acquired. In other words, to avoid deceptive results, trend analysis is determined relative to the other acquisition dates and not in between dates. Results of vegetation trend detected here cannot be extrapolated to change in species composition. Overall image difference as well as cover-type image difference results in measurable VI values (e.g., biomass) and not necessarily species composition change. Although changes seen in image differences might be related to composition change, such assumptions are not appropriate here.

These cover dynamics approaches allow for the identification of ecological status (e.g., gross vegetation trends and their spatial distribution over a landscape). Patterns and critical time intervals were identified in both approaches (overall and cover type, and unsupervised classification approach). Areas of stability versus instability and areas that reacted differently than expected

were identified to define a better management plan; stable
areas may need less management than unstable areas while
certain areas of interest may be studied more intensely to
learn why they react the way they do. It was possible to
define vegetation trend beyond the difference image
approach; areas were not simply classified into negative or
positive trend, but were classified and visually represented
by their spectral signatures. This not only defines areas
that may need more intensive management, but it also
provides information about the entire landscape in the
present as well as in the past that could allow managers to
understand and manage the land better.

Cover-type difference images (Figures 18-24) can be
used to provide information for fire behavior prediction.
Cover-type difference images reveal areas of certain cover
types that have increased or decreased in biomass since
1973. This knowledge along with fuel load by cover type
(Godfrey, 1995) can be used to determine possible areas of
high fire risk. If appropriate decisions are made, fire
management and risk assessment can be enhanced using these
data.

Land cover/land use classification (Figure 9), overall

(Figure 16), and cover type image differences (Figures 18-

24) can be used to facilitate wildlife and livestock

management. The land cover/land use classification can help

determine the amount and distribution of habitat for

wildlife. SAVI images can be used to estimate productivity

(Tucker et al., 1985), vegetation trend, and range condition

(Pickup and Nelson, 1984; Pickup and Chewings, 1988).

This approach to vegetation analysis increases

knowledge of and generates questions about the landscape by

defining new, large-scale ecological patterns on the ground.

Understanding why these and other patterns have developed

will increase ecosystem knowledge and provide land managers

with a more informed basis for making management decisions.

This approach to land cover dynamics provides a new method

for discriminating landscape patterns, which can increase

scientific knowledge and land management options. It allows

for coarse-level analysis and management, and is easily tied

to site-specific surveys in a GIS to provide a comprehensive

ecosystem management plan to be realized.

REFERENCES

Bailey, R. G., 1983. Delineation of ecosystem regions. *Environmental Management.* 7(4):365-373.

Bailey, R. G., 1985. The factor of scale in ecosystem mapping. *Environmental Management.* 9(4):271-276.

Bailey, R. G., 1988. Ecogeographical analysis: a guide to the ecological division of land for resource management. U.S.D.A Forest Service, Misc. Publ. 1465. Washington, DC.

Baret, F., and G. Guyot, 1991. Potentials and limits of vegetation indices for LAI and APAR assessment. *Remote Sensing of Environment,* 35:161-173.

Blaisdell, J. P., 1958. Seasonal development and yield of native plants in the upper Snake River Plains and their relation to certain climatic factors. U.S.D.A. Forest Service, Technical Bulletin, 1190. 68 pp.

Bouman, B. A. M., 1992. Accuracy of estimating the leaf area index from vegetation indices derived from crop reflectance characteristics, a simulation study. *Int. J. Remote Sensing,* 13(16):3069-3084.

Brooks, K. N., P. F. Folliott, H. M. Gregersen, and J. L. Thames, 1991. *Hydrology and the Management of Watersheds*. Iowa State University Press, Ames, Iowa.

Campbell, J. B., 1987. *Introduction to Remote Sensing*. Guilford Press, New York, New York.

Clements, F. E., 1936. Nature and structure of the climax. *Journal of Ecology*, 24:252-284.

Colwell, J. E., 1974. Vegetation canopy reflectance. *Remote Sensing of Environment*, 3:175-183.

Chavez, P. S., 1975. Atmospheric, solar, and M. T. F. corrections for ERTS digital imagery. *Proceedings of the American Society of Photogrammetry*, pp. 69-69a.

Chavez, P. S., Jr. 1988. An improved dark-object subtraction technique for atmospheric scattering correction of multispectral data. *Remote Sensing of Environment*, 24:459-479.

Chavez, P. S., Jr., 1989. Radiometric calibration of Landsat Thematic Mapper multispectral images. *Photogrammetric Engineering and Remote Sensing*, 55(9):1285-1294.

Crist, E. P., and R. C. Cicone, 1984. Comparisons of the

dimensionality and features of simulated Landsat-4 MSS
and TM data. *Remote Sensing of Environment*, 14:235-246.

Deering, D. W., J. W. Rouse, R. H. Haas, and J. A. Schell,
1975. Measuring forage production of grazing units from
Landsat MSS data. *Proceedings of the 10th International
Symposium on Remote Sensing of Environment*, 2:1169-1178.

Dugas, W. A. Jr, 1980. Climatic modeling of phenology,
growth, and production on summer rangelands in Utah and
Montana. PhD Dissertation, Utah State University,
College of Agricultural Science, Dept. of Soil Science
and Biometeorology, 265 pp.

Eidenshink, J. C., 1992. The North American vegetation index
map. TGS Technology, Inc. Work performed under U.S.
Geological Survey contract 14-08-0001-22521.

Franklin, S. E., 1989. Ancillary data input to satellite
remote sensing of complex terrain phenomena. *Computers
and Geosciences*, 15(5):799-808.

Franklin, S. E., and D. R. Peddle, 1987. Texture analysis
of digital image data using spatial cooccurrence.
Computers and Geosciences, 13(3):293-311.

Franklin, S. E., and B. A. Wilson, 1991. Spatial and

spectral classification of remote-sensing imagery.
Computers and Geosciences, 17(8):1151-1172.

Gausman, H. W., 1974. Leaf reflectance of near-infrared.
Photogrammetric Engineering and Remote Sensing,
40(2):183-191.

Gleason, H. A., 1926. The individualistic concept of the
plant Association. Bull. Torrey Bot. Club, 53(1):906-
110.

Godfrey, J. E., 1995. Fire occurrence and behavior and the
effect of fire on deer mouse density in oakbrush on
Camp Williams National Guard Base, Utah. Thesis for
Master of Science, Utah State University, College of
Natural Resources, Dept. of Forest Resources, 66 pp.

Goetz, A. F., J. B. Wellman, and W. L. Barnes, 1985. Optical
remote sensing of the Earth. *Proceedings of the IEEE*,
73(6):950-969.

Gong, P., E. F. Ledrew, and J. R. Miller, 1992.
Registration-noise reduction in difference images for
change detection. *Int. J. of Remote Sensing*, 13(4):773-
779.

Hallum, C., 1993. A change detection strategy for

monitoring vegetation and land-use cover types using
remotely-sensed, satellite-based data. *Remote Sensing of Environment*, 43:171-177.

Hamza, A., 1986. Remote sensing for developing countries: A case study of Tunisia. *Int. J. of Remote Sensing*, 7(2):283-286.

Holm, R. G., M. S. Moran, R. D. Jackson, P. N. Slater, B. Yuan, and S. F. Biggar, 1989. Surface reflectance factor retrieval from Thematic Mapper data. *Remote Sensing of Environment*, 27:47-57.

Huete, A. R., 1987. Soil and sun angle interactions on partial canopy spectra. *Int. J. of Remote Sensing*, 8:1307-1317.

Huete, A. R., 1988. A soil-adjusted vegetation index (SAVI). *Remote Sensing of Environment*, 25:295-309.

Huete, A. R., and R. Escadafal, 1991. Assessment of biophysical soil properties through spectral decomposition techniques. *Remote Sensing of Environment*, 35:149-159.

Huete, A. R., and R. D. Jackson, 1987. Suitability of spectral indices for evaluating vegetation

characteristics on arid rangelands. *Remote Sensing of Environment*, 23:213-232.

Huete, A. R., and A. W. Warrick, 1990. Assessment of vegetation and soil water regimes in partial canopies with optical remotely sensed data. *Remote Sensing of Environment*, 32:155-167.

Huete, A. R., R. D. Jackson, and D. F. Post, 1985. Spectral response of a plant canopy with different soil backgrounds. *Remote Sensing of Environment*, 17:37-53.

Huete, A. R., G. Hua, J. Qi, A. Chehbouni, and W. J. D. van Leeuwen, 1992. Normalization of multidirectional red and NIR reflectances with the SAVI. *Remote Sensing of Environment*, 41:143-154.

Jackson, R. D., 1983. Spectral indices in n-space. *Remote Sensing of Environment*, 13:409-421.

Jackson, R. D., P. N. Slater, and P. J. Pinter Jr., 1983. Discrimination of growth and water stress in wheat by various vegetation indices through clear and turbid atmospheres. *Remote Sensing of Environment*, 13:187-208.

Jensen, J. R., 1986. *Introductory Digital Image Processing: A Remote Sensing Perspective*. Prentice-Hall, Englewood

Cliffs, New Jersey.

Kalcic, M., 1980. A 'non-technical' discussion of principal components and the Kauth-transformation as applied to Landsat data. NASA, Earth Resources Laboratory, ERL Report No. WC-001.

Kauth, R. J. and G. S. Thomas, 1976. The tasseled cap-A graphic description of the spectral-temporal development of agricultural crops as seen by Landsat. *Proceedings of Remotely Sensed Data*, Purdue University, West Lafayette, Indiana, pp. 41-57.

Kessler, W. B., H. Salwasser, C. W. Cartwright, Jr., and J. A. Caplan, 1992. New perspectives for sustainable natural resources management. *Ecological Applications*, 2(3):221-225.

Kimes, D. S., 1983. Dynamics of directional reflectance factor distributions for vegetation canopies. *Applied Optics*, 22(9):1364-1372.

Knipling, E. B., 1970. Physical and physiological basis for the reflectance of visible and near-infrared radiation from vegetation. *Remote Sensing of Environment*, 1:155-159.

Küchler, A. W., 1964. Potential natural vegetation of the
conterminous United States [map]. American Geographical
Society, New York, New York.

Li, Y., T. H. Demetriades-Shah, E. T. Kanemasu, J. K.
Shultis, and M. B. Kirkham, 1993. Use of second
derivatives of canopy reflectance for monitoring prairie
vegetation over different soil backgrounds. *Remote
Sensing of Environment*, 44:81-87.

Markham, B. L., and J. L. Barker, 1987. Radiometric
properties of U.S. processed Landsat MSS data. *Remote
Sensing of Environment*, 22:39-71.

Moran, M. S., R. D. Jackson, P. N. Slater, and P. M.
Teillet, 1992. Evaluation of simplified procedures for
retrieval of Landsat surface reflectance factors from
satellite sensor output. *Remote Sensing of Environment*,
41:169-184.

Neldner, V. J., and C. J. Howitt, 1991. Comparison of an
intuitive mapping classification and numerical
classifications of vegetation in south-east Queensland,
Australia. *Vegetatio*, 94:141-152.

O'Neill, R. V., D. L. DeAngelis, J. B. Waide, and T. F. H.

Allen, 1986. *A Hierarchial Concept of Ecosystems.*

Princeton University Press, Princeton, New Jersey.

Perry, C. R., Jr., and L. F. Lautenschlager, 1984.

Functional equivalence of spectral vegetation indices.

Remote Sensing of Environment, 14:169-182.

Pickup, G., and V. H. Chewings, 1988. Forecasting patterns

of soil erosion in arid lands from Landsat MSS data.

Int J. of Remote Sensing, 9(1):69-84.

Pickup, G., V. H. Chewings, and D. J. Nelson, 1993.

Estimating changes in vegetation cover over time in arid

rangelands using Landsat MSS data. *Remote Sensing of

Environment*, 43:243-263.

Pickup, G., and D. J. Nelson, 1984. Use of Landsat radiance

parameters to distinguish soil erosion, stability, and

deposition in arid central Australia. *Remote Sensing of

Environment*, 16:195-209.

Price, K. P., D. A. Pyke, and L. Mendes, 1992. Shrub

dieback in a semiarid ecosystem: The integration of

remote sensing and geographic information systems for

detecting vegetation change. *Photogrammetric Engineering

and Remote Sensing*, 58(4):455-463.

Qi, J., A. R. Huete, M. S. Moran, A. Chehbouni, and R. D. Jackson, 1993. Interpretation of vegetation indices derived from multi-temporal SPOT images. *Remote Sensing of Environment*, 44:89-101.

Ramsey, R. D., J. D. Born, C. Homer, and T. G. Edwards Jr., 1992. Thematic mapper vegetation mapping for the state of Utah. *Proceedings of the Fourth Forest Service Remote Sensing Applications Conference*, pp. 148-157.

Richardson, A. J., and C. L. Wiegand, 1977. Distinguishing vegetation from soil background information. *Photogrammetric Engineering and Remote Sensing*, 43(12):1541-1552.

Robinove, C. J., 1982. Computation of physical values for Landsat digital data. *Photogrammetric Engineering and Remote Sensing*, 48:781-784.

Rouse, J. W., R. H. Haas, J. A. Schell, and D. W. Deering, 1973. Monitoring vegetation systems in the great plains with ERTS. *Proceedings, Third ERTS Symposium*, 1:48-62.

Sellers, P. J., 1985. Canopy reflectance, photosynthesis and transpiration. *Int. J. of Remote Sensing*, 6(8):1335-1372.

Sellers, P. J., 1987. Canopy reflectance, photosynthesis and transpiration. II. The role of biophysics in the linearity of their interdependence. *Remote Sensing of Environment*, 21:143-183.

Shultz, L., 1993. The Camp Williams project: Ecosystem-based management and research on a military reservation: Report of the collaborative research team. Non-published paper, Utah State University, College of Natural Resources, Dept. of Forest Resources, 5 pp.

Singh, A., 1985a. Thematic mapper radiometric correction research and development results and performance. *Photogrammetric Engineering and Remote Sensing*, 51(9):1379-1383.

Singh, A., 1985b. Postlaunch corrections for Thematic Mapper 5 (TM-5) radiometry in the Thematic mapper image processing system (TIPS). *Photogrammetric Engineering and Remote Sensing*, 51(9):1385-1390.

Singh, A., 1989. Digital change detection techniques using remotely-sensed data. *Int. J. of Remote Sensing*, 10(6):989-1003.

Slater, P. N., and R. D. Jackson, 1982. Atmospheric effects

on radiation reflected from soil and vegetation as measured by orbital sensors using various scanning directions. *Applied Optics*, 21(21):3923-3931.

Slater, P. N., S. F. Biggar, R. G. Holm, R. D. Jackson, Y. Mao, M. S. Moran, J. M. Palmer, and B. Yuan, 1987. Reflectance-and radiance-based methods for the in-flight absolute calibration of multispectral sensors. *Remote Sensing of Environment*, 22:11-37.

Talzik, D. J., S. D. Warren, V. E. Diersing, R. B. Shaw, R. J. Brozka, C. F. Bagley, and W. R. Whitworth, 1992. U.S. Army land condition-trend analysis (LCTA) plot inventory field methods. USACERL Technical Report N-92/03, Washington, D.C.

Teillet, P. M., 1986. Image correction for radiometric effects in remote sensing. *Int. J. of Remote Sensing*, 7(12):1637-1651.

Tucker, C. J., C. L. Vanpraet, M. J. Sharman, and G. Van Ittersum, 1985. Satellite remote sensing of total herbaceous biomass production in the Senegalese Sahel: 1980-1984. *Remote Sensing of Environment*, 17:233-249.

Urban, L. D., R. V. O'Neill, and H. H. Shugart, Jr., 1987.

Landscape ecology: A hierarchical perspective can help scientists understand spatial patterns. *BioScience*, 37(2):119-127.

Viessman, W, Jr., J. W. Knapp, G. L. Lewis, and T. E. Harbaugh, 1977. *Introduction to Hydrology*. Harper and Row, Publishers, New York, New York.

Webb, L. J., J. G. Tracey, W. T. Williams, and G. N. Lance, 1970. Studies in the numerical analysis of complex rain-forest communities. V. A comparison of the properties of floristic and physiognomic-structural data. *Journal of Ecology*, 58:203-232.

West, N. E., K. McDaniel, E. L. Smith, P. T. Tueller, and S. T. Leonard, 1994. Monitoring and interpreting ecological integrity on arid and semi-arid lands of the western United States. New Mexico Range Improvement Task Force. Las Cruces, New Mexico. Report 37.

APPENDICES

APPENDIX A

RADIOMETRIC CALIBRATION

These are the formula for absolute radiometric calibration,
atmospheric correction and sun angle correction for both
Landsat Thematic Mapper (TM) and Mulitspectral Scanner
(MSS). The equations were taken out of EOSAT Landsat
Technical notes from August 1986. For further information
about radiometric calibration read the following references
Markham and Barker, 1983; 1985; 1987, Chavez, 1989,
Robinove, 1982, Teillet, 1986, Holm et al., 1987, and Moran
et al., 1992). Radiance output in mW/cm2*ster*μm and
reflectance is unitless. Information for 1993 TM image:

Band	Gain (Lmax)	Bias or Offset (Lmin)	Bandwidth (μm)
1	1.05525	-0.00761	0.07
2	2.60320	-0.01333	0.08
3	1.63246	-0.01035	0.06
4	2.94300	-0.02227	0.14
5	0.68423	-0.00429	0.20
7	0.42530	-0.00287	0.27

Gains and biases were read off of header file. They are in
mW/cm2*ster and need to be converted to mW/cm2*ster*μm.
Bandwidths were taken from EOSAT Technical Notes Aug., 1986
table 7. These values were put in equation 1 below
(equation 5 in EOSAT Tech. Notes).

Equation 1:   Ln = BWn * L , where

   L = Spectral Radiance in mW/cm2*ster*μm,

   BWn = Nominal bandwidth in μm, and

   Ln = In band radiance in mW/cm2*ster.

The gains and biases were put into equation 1 to convert
them to in band radiance in mW/cm2*ster*μm and are:

Band	Gain	Bias
	(Lmax)	(Lmin)
1	15.075000	-0.108700
2	32.540000	-0.166630
3	27.207670	-0.172500
4	21.021428	-0.159071
5	3.421150	-0.021450
7	1.575185	-0.010629

These are the Lmin and Lmax used in equation 2 below for

calculating L (from EOSAT Tech. Notes, Aug., 1986):

Equation 2: L = Lmin + (Lmax - Lmin / Qcalmax) * Qcal,

where

> L = Spectral Radiance in mW/cm2*ster*μm,
>
> Lmin = Bias in mW/cm2*ster*μm,
>
> Lmax = Gain in mW/cm2*ster*μm,
>
> Qcalmax = maximum Digital number (255 for TM and 63 or
>
> 127 for MSS), and
>
> Qcal = Digital number (value of pixel being converted)

To calculate spectral reflectance R, the following equation

3 was used (Chavez, 1989; Teillet, 1986; Slater et al.,

1987; and Moran et al., 1992):

Equation 3:

R = (* d ^{2} (Lmin + (((Lmax - Lmin) / (Qcalmax) * (Qcal -

H))) / (E * cos((* 2 *) /   360))) * 100, where

> R = Spectral Reflectance in % (0-100),
>
> Lmin = Bias in mW/cm2*ster*μm,
>
> Lmax = Gain in mW/cm2*ster*μm,

Qcalmax = maximum Digital number (255 for TM and 63 or
127 for MSS),

Qcal = Digital number (value of pixel being converted)

$\quad$ = hemispherical / bi-directional reflectance,

d = earth sun distance in astronomical units

(assume = 1),

H = atmospheric haze correction (left bias histogram
method (Jensen, 1986)),

E = solar exoatmospheric irradiance at the sensor from
Table 3, Markham and Barker (1987),

$\quad$ = zenith angle

cos = cosine zenith angle correction or sine of
elevation angle,

2/360 = radians to degrees correction (Erdas defaults
to radians), and

100 = to scale values from decimals to % (use no scale
in Algebra module of Erdas).

Equation 3 was used to radiometrically calibrate all five
images. The equations that were put into Algebra module of
Erdas were:

For 1993 TM,

1: (pi * (-0.1087+(((15.075 + 0.1087)/(255)*(x1-51))) /
(195.7*cos((33*2*pi)/360)))*100

2: (pi * (-0.16663+(((32.54 + 0.16663)/(255)*(x2-19))) /
(182.9*cos((33*2*pi)/360)))*100

3: (pi * (-0.1725+(((27.20767 + 0.1725)/(255)*(x3-17))) /
(155.7 *cos((33*2*pi)/360)))*100

4: (pi * (-0.159071+(((21.021428+0.159071)/(255)*(x4-
12)))/(104.7*cos((33*2*pi)/360)))*100

5: (pi * (-0.02145+(((3.42115 + 0.02145)/(255)*(x5-
10)))/(21.93*cos((33*2*pi)/360))) *100

7: (pi * (-0.010629+(((1.575185 + 0.010629)/(255)*(x7-
3)))/(7.452*cos((33*2*pi)/360))) *100

for 1988 TM,

1: (pi * (-0.24209+(((15.13537 + 0.24209)/(255)*(x1-62))) /
(195.7*cos((39*2*pi)/360)))*100

2: (pi * (-0.52256+(((32.64899 + 0.52256)/(255)*(x2-12))) /
(182.9*cos((39*2*pi)/360)))*100

3: (pi * (-0.4371+(((27.3277 + 04371)/(255)*(x3-19))) /

(155.7*cos((39*2*pi)/360)))*100

4: (pi * (-0.42322+(((21.07016 + 0.42322)/(255)*(x4-9))) /

(104.7*cos((39*2*pi)/360)))*100

5: (pi * (-0.08274+(((3.41944 + 0.08274)/(255)*(x5-9))) /

(21.93*cos((39*2*pi)/360)))*100

7: (pi * (-0.031585+(((1.572989 + 0.031585/(255)*(x7-6))) /

(7.452*cos((39*2*pi)/360)))*100

for 1980 MSS,

1: (((((x1-14)/127)*(26.3-0.8))+0.8)*(pi/(185.6*

cos((32*2*pi) /360))))*100

2: (((((x2-11)/127)*(17.6-0.6))+0.6)*(pi/(155.9*

cos((32*2*pi)/360))))*100

3: (((((x3-12)/127)*(15.2-0.6))+0.6)*(pi/(126.9*

cos((32*2*pi)/360))))*100

4: (((((x4-5)/127)*(13.0-0.4)+0.4)*(pi/(90.6*

cos((32*2*pi)/360))))*100

for 1975 MSS,

1: `(((((x1-12)/127)*(21.0-1.0))+1.0)*(pi/(185.6*`
`cos((31*2*pi)/360))))*100`

2: `(((((x2-12)/127)*(15.6-0.7))+0.7)*(pi/(155.9*`
`cos((31*2*pi)/360))))*100`

3: `(((((x3-21)/127)*(14.0-0.7))+0.7)*(pi/(126.9*`
`cos((31*2*pi)/360))))*100`

4: `(((((x4-7)/63)*(13.8-0.5)+0.5)*(pi/(90.6*`
`cos((31*2*pi)/360))))*100`

for 1973 MSS,

1: `(((((x1-5)/127)*(24.8-0.0))+0.0)*(pi/(185.2*`
`cos((29*2*pi)/360))))*100`

2: `(((((x2-14)/127)*(20.0-0.0))+0.0)*(pi/(158.4*`
`cos((29*2*pi)/360))))*100`

3: `(((((x3-12)/127)*(17.6-0.0))+0.0)*(pi/(127.6*`
`cos((29*2*pi)/360))))*100`

4: `(((((x4-1)/63)*(15.3-0.0)+0.0)*(pi/(90.4*`
`cos((29*2*pi)/360))))*100.`

*NOTE: 1988 header file was lost, so I used Lmin and Lmax from EOSAT fast format document table 1 that came with the 1993 image not EOSAT Technical Notes August, 1986 table 2 for 1988 calculations.

APPENDIX B

ANTECEDENT PRECIPITATION INDEX

These formulas are used to calculate the API. The equations was taken from Viessman et al. (1977) pgs. 100 and 101 explaining Kohler and Linsley's equation for individual storms.

$$P_a = b_1 P_1 + b_2 P_2 + \ldots + b_t P_t$$

where

p_a = the antecedent precipitation index

P_1, P_2, and P_t = precipitation which occured a number

of days prior to the calculation date

b_1, b_2, and b_t = constants (less than unity) assumed to

be a function of t.

b_t is considered to be related to t by:

$$b_t = K^t$$

where K is a recession constant (0.85 to 0.98).

I used a recession constant K = 0.9. so for one day prior to the calculation date, K = 0.9. Two days prior, K would be $0.9^2 = 0.81$. Three days prior, K would be $0.9^3 = 0.73$, and so on.

APPENDIX C

ADUSTMENT FACTOR CALCULATION FOR SAVI
BASED ON API

BASED ON APIThe high and low L factors were determined
to be 0.5 and 0.25 respectively. In order to "adjust" for
soil moisture, the L factors were changed in between the
high and low based on the antecedent precipitation index
(API). The year with the highest API value on the date of
satellite acquisition would have an L of 0.25 (lowest
possible L) and the year with the lowest API value would
have an L of 0.5 (the highest possible L). The other years
were related to API as well, and the appropriate L value was
then calculated. The high and low L factors were more or
less arbitrarily defined by the author keeping in mind that
Huete (1988) suggested an L factor of between 0.25 and 1.

The L factors and API's for satellite acquisition were:

Year	API (mm)	L
1993	0.87452	0.5
1988	1.23088	0.496960328
1980	30.1836	0.25
1975	25.3495	0.291233809
1973	3.15951	0.480509538